A structural MRI marker predicts individual differences in impulsivity and classifies patients with behavioral-variant frontotemporal dementia from matched controls

Valérie Godefroy, Anaïs Durand, Marie-Christine Simon, Bernd Weber, Joseph Kable, Caryn Lerman, Fredrik Bergström, Richard Levy, Bénédicte Batrancourt, Liane Schmidt, et al.

▶ **To cite this version:**

Valérie Godefroy, Anaïs Durand, Marie-Christine Simon, Bernd Weber, Joseph Kable, et al.. A structural MRI marker predicts individual differences in impulsivity and classifies patients with behavioral-variant frontotemporal dementia from matched controls. 2024. hal-04728923

HAL Id: hal-04728923
https://hal.science/hal-04728923v1

Preprint submitted on 9 Oct 2024

HAL is a multi-disciplinary open access archive for the deposit and dissemination of scientific research documents, whether they are published or not. The documents may come from teaching and research institutions in France or abroad, or from public or private research centers.

L'archive ouverte pluridisciplinaire **HAL**, est destinée au dépôt et à la diffusion de documents scientifiques de niveau recherche, publiés ou non, émanant des établissements d'enseignement et de recherche français ou étrangers, des laboratoires publics ou privés.

bioRxiv preprint doi: https://doi.org/10.1101/2024.09.12.612706; this version posted September 16, 2024. The copyright holder for this preprint (which was not certified by peer review) is the author/funder, who has granted bioRxiv a license to display the preprint in perpetuity. It is made available under aCC-BY-NC-ND 4.0 International license.

A structural MRI marker predicts individual differences in impulsivity and classifies patients with behavioral-variant frontotemporal dementia from matched controls

Valérie Godefroy[1], Anai□s Durand[2], Marie-Christine Simon[4], Bernd Weber[5], Joseph Kable[6], Caryn Lerman[7], Fredrik Bergström[8,9], Richard Levy[2], Bénédicte Batrancourt[2], Liane Schmidt[2], Hilke Plassmann[2,3]* and Leonie Koban[1]*

Author affiliations:

(1) Université Claude Bernard Lyon 1, CNRS, INSERM, Centre de Recherche en Neurosciences de Lyon CRNL U1028 UMR5292, F-69500, Bron, France ;

(2) Paris Brain Institute (ICM), INSERM U 1127, CNRS UMR 7225, Sorbonne University, Paris, France UMR 7225, Sorbonne University, Paris, France;

(3) Marketing Area, INSEAD, Fontainebleau, France,

(4) Institute for Nutrition Science, University of Bonn, Bonn, Germany;

(5) Center for Economics and Neuroscience, University of Bonn, Bonn, Germany;

(6) Department of Psychology, University of Pennsylvania, Philadelphia, PA, USA;

(7) USC Norris Comprehensive Cancer Center

(8) Faculty of Psychology and Educational Sciences, University of Coimbra, Portugal

(9) Department of Psychology, University of Gothenburg, Sweden

*shared senior authorship

Short title: MRI-BASED PREDICTION OF IMPULSIVITY

bioRxiv preprint doi: https://doi.org/10.1101/2024.09.12.612706; this version posted September 16, 2024. The copyright holder for this preprint (which was not certified by peer review) is the author/funder, who has granted bioRxiv a license to display the preprint in perpetuity. It is made available under aCC-BY-NC-ND 4.0 International license.

Correspondence to: Valérie Godefroy, PhD

Université Claude Bernard Lyon 1, CNRS, INSERM, Centre de Recherche en Neurosciences de Lyon CRNL U1028 UMR5292

CH Le Vinatier, Bât. 462, Neurocampus 95 Bd Pinel - 69675 BRON CEDEX, France

E-mail: vlrgodefroy@gmail.com

And :Leonie Koban, PhD, CRNL, CH Le Vinatier, Bât. 462, Neurocampus 95 Bd Pinel - 69675 BRON CEDEX, France ; email: leonie.koban@cnrs.fr

Acknowledgments

This study was funded by an ANR Tremplin-ERC grant to HP, a Sorbonne Emergence Grant to HP and LK, and an ERC Starting Grant to LK. Study 2 was funded by National Cancer Institute Grants R01-CA-170297 to J.W.K. and C.L. and R35-CA-197461 to C.L. Study 3 was funded by grant ANR-10-IAIHU-06 from the program ‘Investissements d’avenir’, by grant FRM DEQ20150331725 from the foundation ‘Fondation pour la recherche médicale’, and by the ENEDIS company. FB was supported by Fundação para a Ciência e Tecnologia (CEECIND/03661/2017). We thank all the participants and organizers of the three studies mentioned in this paper as well as all the students who contributed to help data collection.

Data availability statement

Deidentified data for the three studies are available at https://figshare.com/s/a090ef2531a7d7b9a2e4 and upon request to the first author.

bioRxiv preprint doi: https://doi.org/10.1101/2024.09.12.612706; this version posted September 16, 2024. The copyright holder for this preprint (which was not certified by peer review) is the author/funder, who has granted bioRxiv a license to display the preprint in perpetuity. It is made available under aCC-BY-NC-ND 4.0 International license.

ABSTRACT

Impulsivity and higher preference for sooner over later rewards (i.e., delay discounting) are transdiagnostic markers of many psychiatric and neurodegenerative disorders. Yet, their neurobiological basis is still debated. Here, we aimed at 1) identifying a structural MRI signature of delay discounting in healthy adults, and 2) validating it in patients with behavioral variant frontotemporal dementia (bvFTD)—a neurodegenerative disease characterized by high impulsivity. We used a machine-learning algorithm to predict individual differences in delay discounting rates based on whole-brain grey matter density maps in healthy male adults (Study 1, N=117). This resulted in a cross-validated prediction-outcome correlation of r=0.35 (p=0.0028). We tested the validity of this brain signature in an independent sample of 166 healthy adults (Study 2) and its clinical relevance in 24 bvFTD patients and 18 matched controls (Study 3). In Study 2, responses of the brain signature did not correlate significantly with discounting rates, but in both Studies 1 and 2, they correlated with psychometric measures of trait urgency—a measure of impulsivity. In Study 3, brain-based predictions correlated with discounting rates, separated bvFTD patients from controls with 81% accuracy, and were associated with the severity of disinhibition among patients. Our results suggest a new structural brain pattern—the Structural Impulsivity Signature (SIS)—which predicts individual differences in impulsivity from whole-brain structure, albeit with small-to-moderate effect sizes. It provides a new brain target that can be tested in future studies to assess its diagnostic value in bvFTD and other neurodegenerative and psychiatric conditions characterized by high impulsivity.

Keywords: brain signature; machine-learning; dementia; decision-making; delay discounting; intertemporal choice; prediction

bioRxiv preprint doi: https://doi.org/10.1101/2024.09.12.612706; this version posted September 16, 2024. The copyright holder for this preprint (which was not certified by peer review) is the author/funder, who has granted bioRxiv a license to display the preprint in perpetuity. It is made available under aCC-BY-NC-ND 4.0 International license.

BACKGROUND

Impulsivity is the tendency to act in a rush and to seek immediate rewards without consideration of potentially negative long-term consequences [1]. Trait impulsivity varies substantially within the general population, with high impulsivity being a hallmark of many psychiatric and neurological conditions [2]. Despite the many negative consequences of high impulsivity for health and life in general [3,4], its neurobiological correlates are still unclear, and it is unknown whether individual differences in impulsivity can be reliably predicted based on structural brain features [5–7]. Neurobiological measures of impulsivity could help to understand the mechanisms and disentangle the heterogeneity of symptoms related to maladaptive behavior and decision-making. Brain signatures of impulsivity could also constitute new targets for diagnosis and treatment. They might aid in the diagnosis and monitoring of conditions such as behavioral variant frontotemporal dementia (bvFTD)—a neurodegenerative disorder characterized by frontal and temporal brain atrophy, with high impulsivity and inappropriate behaviors as core symptoms [8]. In this study, we aimed at developing a structural brain signature of individual differences in impulsivity, and tested whether it could accurately classify patients with bvFTD from matched healthy controls.

The idea that any psychological construct would depend on only one or a few isolated brain regions has been more and more challenged. A new paradigm of “brain signatures” (or “neuromarkers”) promoting a multivariate *brain patterns* view has therefore emerged, to complement the traditional univariate brain mapping approach examining brain regions independently [9]. Brain signatures are predictive models of mental events or of individual variables (such as impulsivity) that take into account distributed information across multiple brain systems [10]. Brain signatures using structural data are increasingly used in the field of translational neuroimaging, especially for applications in patients with neurodegenerative conditions [11]. One of the greatest advantages of these predictive models which predict behavior from brain features is that they can be tested across studies, labs and populations to challenge their generalizability. We used this brain signature approach to identify a network of spatially distributed structural features associated with impulsivity, as measured by delay discounting. The present study applies the “component process” framework of brain signatures [11]. Instead of predicting a given heterogenous condition such as bvFTD, we aimed at identifying a predictive model of a key symptom (i.e., impulsivity), which is a common factor across

bioRxiv preprint doi: https://doi.org/10.1101/2024.09.12.612706; this version posted September 16, 2024. The copyright holder for this preprint (which was not certified by peer review) is the author/funder, who has granted bioRxiv a license to display the preprint in perpetuity. It is made available under aCC-BY-NC-ND 4.0 International license.

different diseases. This framework is also suited to the purpose of predicting a specific patient's clinical profile in a perspective of personalized medicine.

Several arguments support the idea that delay discounting—how much people prefer smaller sooner over larger later rewards—is a reliable measure of stable individual differences in a specific facet of impulsivity (that is the urgency to get short-term rather than long-term reward). Individual differences in delay discounting are relatively stable over time and show significant genetic heritability [12–14]. Delay discounting moreover constitutes a potential transdiagnostic marker of conditions with high impulsivity since it has been found to be altered across multiple psychiatric [15] and neurodegenerative conditions [16]. Recent studies have therefore started to investigate the neurobiological basis of individual differences in delay discounting [7,14,17–23]. However, less is known about how these candidate brain markers of delay discounting are expressed in psychiatric and neurological conditions characterized by increased impulsivity.

Characterized by multiple impulsivity-related symptoms, bvFTD is a good example to demonstrate the clinical potential (in particular for diagnosis) of a structural brain signature of delay discounting. BvFTD is the most common clinical variant of syndromes associated with predominant degeneration of the prefrontal and temporal regions as well as the basal ganglia. It is characterized by significant changes in personality and behavior including disinhibition (socially inappropriate and generally impulsive behaviors), as well as executive function deficits [8]. Brain regions known to be related to delay discounting such as the orbitofrontal cortex (OFC), ventromedial prefrontal cortex (vmPFC) and ventral striatum [24–26] are often affected in bvFTD [27,28]. Relatedly, most studies found an alteration of delay discounting in bvFTD patients compared to controls [16,29–32].

Here, we first trained and cross-validated a structural MRI-based brain signature in a healthy adult population (Study 1, N=117) using LASSO-PCR (least absolute shrinkage and selection operator-principal component regression)—an established machine-learning algorithm [33,34] —to predict individual differences in delay discounting rates from subjects' grey matter maps (N=117). Brain markers of individual differences need to be tested in different and completely independent samples and studies to establish their robustness and generalizability [10]. Thus, in Study 2, we tested the replicability of the brain signature in a second independent sample of healthy adults (N=166). In Study 3, we tested the validity of the structural brain signature in a clinical population of patients with behavioral variant frontotemporal dementia, who often show high impulsivity and were shown to be

bioRxiv preprint doi: https://doi.org/10.1101/2024.09.12.612706; this version posted September 16, 2024. The copyright holder for this preprint (which was not certified by peer review) is the author/funder, who has granted bioRxiv a license to display the preprint in perpetuity. It is made available under aCC-BY-NC-ND 4.0 International license.

steeper discounters (N = 42, including 24 bvFTD patients and 18 matched controls) [35]. If a consistent pattern of grey matter density across the brain can reliably predict delay discounting and more generally impulsivity, then the brain-predicted discounting should be higher in bvFTD patients than in controls and should be related to the level of clinically assessed impulsivity in patients. In addition to testing the generalizability of the brain signature developed in Study 1, we analyzed the topographical distribution of the most important structural alterations contributing to differences of brain-predicted delay discounting.

bioRxiv preprint doi: https://doi.org/10.1101/2024.09.12.612706; this version posted September 16, 2024. The copyright holder for this preprint (which was not certified by peer review) is the author/funder, who has granted bioRxiv a license to display the preprint in perpetuity. It is made available under aCC-BY-NC-ND 4.0 International license.

MATERIALS AND METHODS

Participants

The research reported here complies with all relevant ethical regulations. The study protocols were approved by the institutional review board of Bonn University's Medical School (Study 1), by the University of Pennsylvania Institutional Review Board (Study 2), and by the French Ethics Committee "Comité de Protection des Personnes Sud Méditerranée I" (Study 3).

Study 1

In Study 1, participants were recruited in the context of a seven-week dietary intervention study (https://osf.io/rj8sw/?view_only=af9cba7f84064e61b29757f768a8d3bf) at the University of Bonn in Germany. In this study, only male participants were recruited, with the following inclusion criteria: age between 20 and 60 years, right-handedness, non-smoker, no excessive drug or alcohol use in the past year, no psychiatric or neurological disease, body mass index (BMI) between 20 and 34, no other chronic illness or medication, following a typical Western diet without dietary restrictions, and no MRI exclusion criteria (e.g., large tattoos, metal in the body,). For the present purpose, we used only the behavioral and structural MRI data collected during a baseline session before the dietary intervention. N=117 participants were tested for the baseline session of Study 1. However, four participants were excluded from the present analyses due to being outliers on grey matter density maps (three participants) and due to very incoherent choices at the intertemporal choice task (one participant). Thus, the data of a total of 113 participants was used for the analyses.

Study 2

In Study 2, participants were recruited in the context of a ten-week cognitive training study (registered at clinicaltrials.gov as Clinical trial reg. no. NCT01252966) at the University of Pennsylvania, USA. Individuals between 18 and 35 years of age who reported home computer and internet access were recruited. Exclusion criteria were: an IQ score of <90 on Shipley Institute of Living Scale, self-reported history of neurological, psychiatric, or addictive disorders (excluding nicotine), positive breath alcohol reading (>0.01), color blindness, left-handedness, and claustrophobia. Here, we focused on behavioral and structural MRI data collected during the baseline session before the cognitive training. In Study 2, N=166 participants (mean age=24.5, 59% male) were included in the baseline session and all were included in our data analyses.

bioRxiv preprint doi: https://doi.org/10.1101/2024.09.12.612706; this version posted September 16, 2024. The copyright holder for this preprint (which was not certified by peer review) is the author/funder, who has granted bioRxiv a license to display the preprint in perpetuity. It is made available under aCC-BY-NC-ND 4.0 International license.

Study 3

For Study 3, participants were recruited in the context of a clinical study at the Paris Brain Institute, France (clinicaltrials.gov: NCT03272230). This study was designed to investigate the behavioral correlates and neural bases of neuropsychiatric symptoms associated with behavioral variant frontotemporal dementia (bvFTD). BvFTD patients were recruited in two tertiary referral centers, at the Pitié-Salpe□trière Hospital and the Lariboisière Fernand-Widal Hospital, in Paris. Patients were diagnosed according to the International Consensus Diagnostic Criteria [8]. To be included, bvFTD patients had to present a Mini-Mental State Evaluation (MMSE) score of at least 20. Healthy controls (HC) were recruited by an online announcement. Inclusion criteria included a MMSE score of at least 27 and matching the demographic characteristics of the bvFTD group. In total, 24 bvFTD patients (mean age=66.6, 66.6% male) and 18 controls matched to patients for age and sex (mean age=62.6, 44.4% male) were recruited in this clinical study (see Supplementary table 1). Data of all participants were used for our analyses.

Intertemporal choice tasks

Study 1

During the intertemporal choice (ITC) task performed in an MRI scanner, participants in Study 1 were presented with 108 trials offering a choice between a smaller sooner (SS) reward option and a larger later (LL) reward option [14]. Participants were informed that one of their choices could be paid out at the end of the experiment, which made their choices non-hypothetical and incentive-compatible. The two options were displayed on the left or right of the screen (position randomized) for 4 seconds. Participants used their left or right index finger to press the response key corresponding to their choice (left index for left option or right index for right option). The option chosen by the participant was then highlighted by a yellow frame which remained on the screen until the end of the 4 second trial. Trials were presented in randomized order (see Koban et al., 2023 for further details on the trial structure).

Study 2

During the ITC performed in an MRI scanner, participants had to make 120 choices between the same smaller immediate reward ($20 today) and a varying larger reward available after a longer delay (e.g., $40 in a month) [36]. Participants were informed that one of their choices could be paid out at the end of the experiment, which made their choices non-hypothetical and incentive-compatible. Each trial

bioRxiv preprint doi: https://doi.org/10.1101/2024.09.12.612706; this version posted September 16, 2024. The copyright holder for this preprint (which was not certified by peer review) is the author/funder, who has granted bioRxiv a license to display the preprint in perpetuity. It is made available under aCC-BY-NC-ND 4.0 International license.

started with the presentation of the amount and delay of the larger later option. Once subjects had made their choice, a checkmark on the screen indicated if the larger later option was chosen and a "X" indicated that the immediate option was chosen for 1 s. Subjects had 4 s to make their choice.

Study 3

In Study 3, participants performed two ITC tasks on a computer screen, one using monetary rewards (from 8 to 35 euros) and one using food rewards (from 8 to 35 chocolates) in randomized order [35]. In this study, using these two tasks allowed us to test the validity of our brain signature for the prediction of discounting of several types of reward, and thus to investigate generalizability across reward domains. Each of these tasks included 32 choices between SS and LL options. Participants were instructed that one of their 32 choices could be randomly selected and the option that they had chosen would be given to them. Thus, like in Study 1 and 2, participants' choices were non-hypothetical and incentive-compatible. For each trial, participants could indicate their choice by pressing either a blue key on the keyboard with their right-hand index to select the option on the left or a yellow key with their right-hand middle finger to select the option on the right. Once the choice had been made, a message on the screen indicated which option had been chosen. Trials were presented in randomized order.

Other measures of impulsivity traits and symptoms

Study 1

In Study 1, along with choice data collected from the ITC task, we used self-report data from the Impulsive Behavior Short Scale–8 (I-8), which measures the psychological construct of trait impulsivity according to the Urgency, lack of Premeditation, lack of Perseverance, and Sensation seeking (UPPS) model with four subscales comprising two items each [37]. We predicted that the trait of *urgency—defined as the tendency to act rashly in an emotional context* (e.g., "I sometimes do things to cheer myself up that I later regret")— would be closest to brain-predicted delay discounting, as both urgency and delay discounting are supposed to measure a tendency to prefer most immediate rewards at the expense of potential long-term gains.

Study 2

In Study 2, we used data from the UPPS-P Impulsive Behavior Scale, which measures trait impulsivity according to the UPPS model with five subscales: positive urgency, negative urgency, lack of premeditation, lack of perseverance, and sensation seeking [38]. Paralleling Study 1, we predicted that

bioRxiv preprint doi: https://doi.org/10.1101/2024.09.12.612706; this version posted September 16, 2024. The copyright holder for this preprint (which was not certified by peer review) is the author/funder, who has granted bioRxiv a license to display the preprint in perpetuity. It is made available under aCC-BY-NC-ND 4.0 International license.

urgency would be the most closely related to brain-based predictions. We used the average of the subscales of positive urgency (rash actions taken in response to positive emotional states) and negative urgency (rash actions taken in response to negative emotional states) to test this hypothesis.

Study 3

This clinical study did not include a trait measure of impulsivity such as the UPPS scale. However, clinical measures of core symptoms of bvFTD were available, in particular for two symptoms closely related to impulsivity: inhibition deficit and dysexecutive syndrome (i.e., dysfunction in executive functions). In another recent investigation of the same sample, we found that these two bvFTD symptoms are related to higher discounting rates of both money and food [35]. We further used the Hayling Sentence Completion Test (HSCT) [39] considered as an objective measure of inhibition deficit, and the Frontal Assessment Battery (FAB) [40] as a measure of executive functions (lower scores indicating worse executive functions). In the HSCT, participants are asked to complete 15 sentences using the appropriate word, as fast as possible (automatic condition, part A), and 15 sentences using a completely unrelated word (inhibition condition, part B). We used the Hayling error score (number of errors in part B) as a measure of the difficulty to inhibit a prepotent response, as in Flanagan et al. [41].

MRI data acquisition and preprocessing

Study 1

Brain imaging data for Study 1 were acquired using a Siemens Trio 3T scanner. Structural images were acquired using a T1 weighted MPRAGE sequence with the following parameters: TR 1660 ms; TE 2.54 ms; FoV 256 mm; 208 slices; slice thickness 0.80 mm; TI 850 ms; flip angle 9°; voxel size 0.8 mm isomorphic; total acquisition time 6:32 min. T1 images were preprocessed for Voxel Based Morphometry (VBM) analyses with SPM 12. We used the SPM module “Segment” for segmentation, bias correction and rigid alignment of T1 images. These images were then used as input into the DARTEL SPM module to create a customized DARTEL template and individual ‘flow fields’ for each subject. DARTEL determines the nonlinear deformations for warping all grey and white matter images so that they match each other. Finally, the SPM module “Normalise to MNI space” generated spatially normalized grey matter images using the deformations estimated in the previous step and images were spatially smoothed with a 6 mm Gaussian FWHM kernel. Among the obtained grey matter

bioRxiv preprint doi: https://doi.org/10.1101/2024.09.12.612706; this version posted September 16, 2024. The copyright holder for this preprint (which was not certified by peer review) is the author/funder, who has granted bioRxiv a license to display the preprint in perpetuity. It is made available under aCC-BY-NC-ND 4.0 International license.

images, three outliers (based on Mahalanobis distance of individual grey matter density maps with Bonferroni correction) were detected and excluded from further analyses.

Study 2

Brain imaging data for Study 2 were acquired using a Siemens Trio 3T scanner (with a 32-channel head coil). Structural images were acquired using a T1 weighted MPRAGE sequence with the following parameters: TR 1630 ms; TE 3.11 ms; FOV 192x256; 160 slices; slice thickness 1 mm; TI 1100 ms; flip angle 15°; voxel size 0.9375 × 0.9375 × 1.000 mm; total acquisition time 4:35 min. We used existing data preprocessed by Kable and colleagues [36]. T1 images were preprocessed for VBM analyses using the default preprocessing pipeline of the Computational Anatomy Toolbox (CAT12) for SPM12. T1-weighted images underwent spatial adaptive non-local means (SANLM) denoising filter, were bias corrected, and affine-registered, followed by standard SPM unified tissue segmentation into grey matter, white matter, and cerebral spinal fluid. The grey matter volume images were spatially registered to a common template using Geodesic Shooting, resampled to 1.5 mm3, and spatially smoothed with an 8 mm Gaussian FWHM kernel.

Study 3

Brain imaging data for Study 3 were acquired using a Siemens Prisma whole-body 3T scanner (with a 12-channel head coil). Structural images were acquired using a T1 weighted MPRAGE sequence with the following parameters: TR 2400 ms; TE 2.17 ms; FOV 224 mm; 256 slices; slice thickness 0.70 mm; TI 1000 ms; flip angle 8°; voxel size 0.7 mm isomorphic; total acquisition time 7:38 min. T1 images were preprocessed for Voxel Based Morphometry (VBM) analyses using SPM 12, following the same steps as in Study 1.

Data analyses

The analyses detailed in the following subsections aimed to: (1) develop and validate a structural brain signature predicting delay discounting in a healthy population (Study 1); (2) test the validity of predictions of this structural brain signature as measures of impulsivity in independent studies involving different types of populations, including healthy (Study 2) and clinical samples (Study 3). All analyses were performed using R Studio (1.2.1335) and Matlab (R2017b). The global analytic approach is summarized in Figure 1A. The specific analyses conducted in each study to check the validity of brain-based predictions are detailed in Figure 1B.

bioRxiv preprint doi: https://doi.org/10.1101/2024.09.12.612706; this version posted September 16, 2024. The copyright holder for this preprint (which was not certified by peer review) is the author/funder, who has granted bioRxiv a license to display the preprint in perpetuity. It is made available under aCC-BY-NC-ND 4.0 International license.

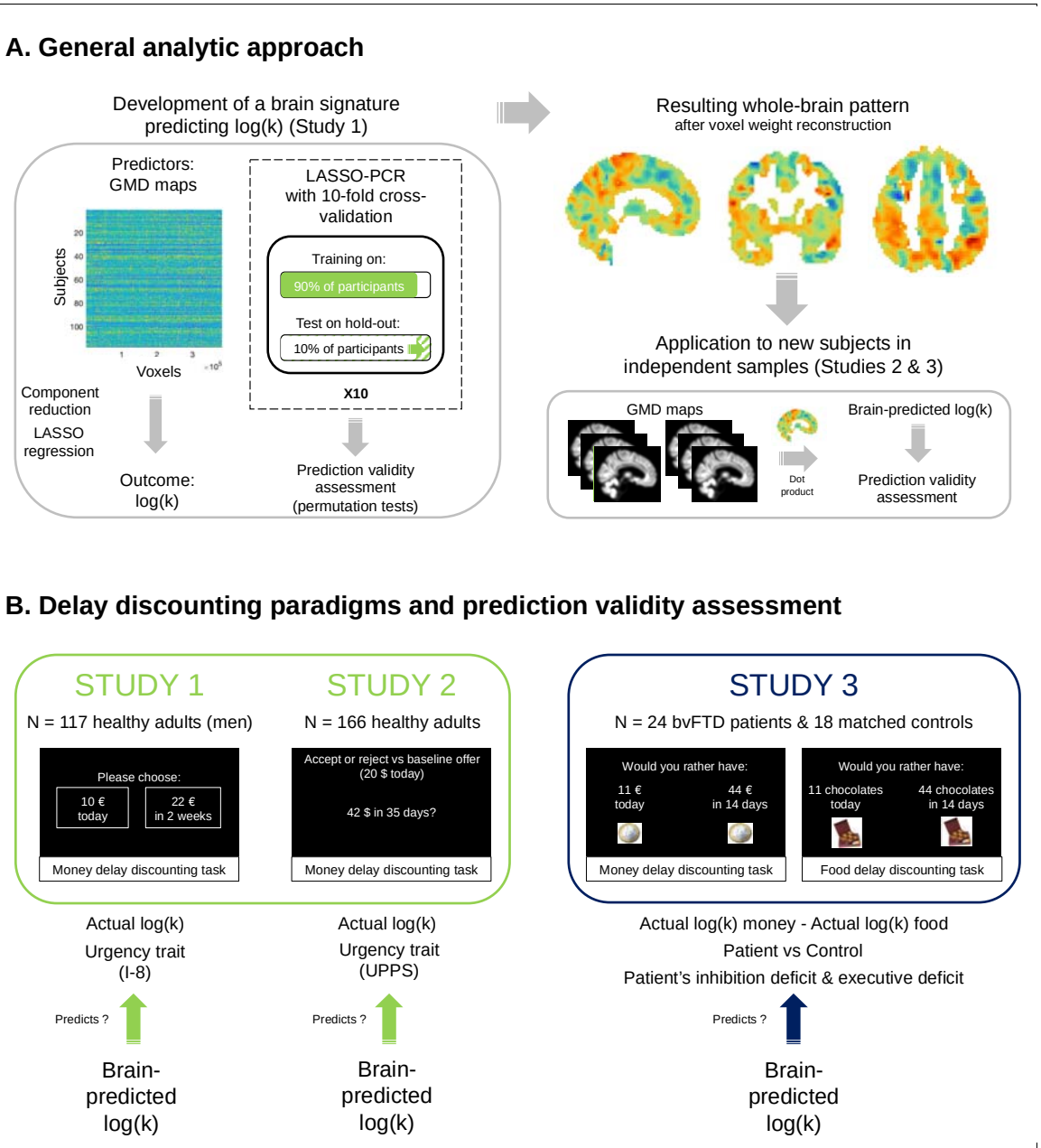

Figure 1. Methodological approach for the development and validation of a structural brain signature of impulsivity. A) Grey matter density (GMD) maps from healthy participants of Study 1 were used for the prediction of delay discounting (log(k)) by LASSO-PCR with 10-fold cross-validation. In each fold, the classifier was trained on 90% of the data and tested on the remaining 10% hold-out data to evaluate its predictive accuracy. The predictive whole-brain pattern obtained from Study 1 was then tested in two independent samples, on the data of participants of Study 2 (healthy participants), and Study 3 (patients with neurodegenerative dementia and matched healthy control participants). The brain pattern was applied to the grey matter density maps of each study's participants to evaluate the validity of its predictions in different types of population. **B)** Several tests were performed in each of the four studies to assess the validity of the structural signature trained and cross-validated in

bioRxiv preprint doi: https://doi.org/10.1101/2024.09.12.612706; this version posted September 16, 2024. The copyright holder for this preprint (which was not certified by peer review) is the author/funder, who has granted bioRxiv a license to display the preprint in perpetuity. It is made available under aCC-BY-NC-ND 4.0 International license.

Study 1. In Study 1 (the training and cross-validation sample), permutation tests on different metrics (MSE, RMSE, MAE) and in particular on the correlation between predicted and actual log(k) were used to investigate the predictive accuracy of the developed brain pattern; the validity of predictions was also assessed through testing their correlation with out-of-sample log(k) measured several weeks later and with a self-report measure of the urgency component of impulsivity trait (subscale of Impulsive Behavior Short Scale). Study 2 and 3 served as independent test samples to further validate and generalize the structural signature developed in Study 1. In Study 2, we tested whether brain-based predictions correlated with the actual log(k)'s computed in the sample and with self-reported urgency trait (mean of positive and negative urgency subscales of UPPS- Impulsive Behavior Scale). In Study 3, which involved patients with behavioral variant frontotemporal dementia (bvFTD) matched with healthy controls, we tested: 1) correlations between the brain pattern predictions and observed delay discounting for two types of stimuli (money and food) across patients and controls; 2) the ability of brain-based predictions to distinguish patients from controls; 3) correlations between measures of impulsivity symptoms (inhibition and executive deficits) and brain-based predictions among patients.

Computation of discount rates

In all three studies, the individual discounting rate (k) was estimated by fitting logistic regressions to the individual choice data, with the assumption that the subjective value (SV) of the choice options followed hyperbolic discounting, as follows:

$$SV = \frac{A}{1 + kD}$$

where A is the amount of the option, D is the delay until the receipt of the reward (for immediate choice, D = 0), and k is a discounting rate parameter that varies across subjects. Higher values of k indicate greater discounting and thus higher preference for sooner rewards. In Study 1, we used logistic regressions (as described in Wileyto et al., 2004) to estimate the individual parameter k from the participant's answers in the ICT task at baseline and we used the log(k) values as the parameter to be predicted. Individual k's were log-transformed in all studies to obtain non-skewed distributions of discounting parameters. In Study 2, we also used the log(k) values at baseline (see [36]). In Study 3, we used the log(k) values calculated in bvFTD patients matched with controls for both monetary and food rewards (see [35]).

LASSO-PCR, training and cross-validation of the brain pattern predicting log(k) in Study 1

We used a regression-based standard machine learning algorithm, LASSO-PCR (least absolute shrinkage and selection operator-principal component regression) [34], to train a classifier to predict

bioRxiv preprint doi: https://doi.org/10.1101/2024.09.12.612706; this version posted September 16, 2024. The copyright holder for this preprint (which was not certified by peer review) is the author/funder, who has granted bioRxiv a license to display the preprint in perpetuity. It is made available under aCC-BY-NC-ND 4.0 International license.

log(k) from the individual whole brain grey matter density (GMD) maps. LASSO-PCR uses principal components analysis (PCA) to reduce the dimensionality of the data and LASSO regression to predict the outcome (log(k)) from the extracted component scores. The components identified by the PCA correspond to groups of brain regions that covary with each other in terms of grey matter density. The LASSO algorithm fits a regularized regression model predicting log(k) from the identified components. This algorithm iteratively shrinks the regression weights towards zero, thus selecting a subset of predictors and reducing the contribution of unstable components. LASSO-PCR is suited to make predictions from thousands of voxels across the whole-brain, in particular because it solves the issue of multicollinearity between voxels and brain regions (see [43,44]). Moreover, it is possible to reconstruct voxel weights across the brain (from voxel loadings on PCA components and LASSO regression coefficients of components), yielding predictive brain maps that are easier to interpret than component weights. To assess the accuracy of this predictive modeling from GMD maps, we used a 10-fold cross-validation process. The brain classifier was trained on 90% of the data and tested on the remaining 10% with 10 iterations, so that each participant was used for training the model in nine folds and for testing the accuracy of its prediction in the remaining fold. Ten-fold cross-validation is within the range of typically recommended folds (between 5 and 10) and allowed for a large training sample size at each iteration [45,46]. Default regularization parameters were used for all machine-learning analyses to avoid overfitting of the model to the data. We used four metrics to assess the accuracy of the model predictions: the mean squared error (MSE) of prediction, the root mean squared error (RMSE), the mean absolute error (MAE), and the correlation between the model predictions (from the 10 hold-out test samples) and observed log(k)'s (prediction-outcome correlation).

Test of the validity of predicted log(k) in Study 1

To test the reliability of the predictions, we used permutation tests assessing the statistical significance of the accuracy metrics (MSE, RMSE, MAE and prediction-outcome correlation). More precisely, 5000 iterations of randomly permuting the log(k) values were used to generate null distributions of these four metrics and thus to assess the probability of: (MSE < actual MSE), (RMSE < actual RMSE), (Mean abs. error < actual Mean abs. error) and of (prediction-outcome correlation < actual prediction-outcome correlation) under the null hypothesis. To further confirm the validity of out-of-sample predictions of log(k), we performed correlation tests between the predicted log(k) and: (1) calculated

bioRxiv preprint doi: https://doi.org/10.1101/2024.09.12.612706; this version posted September 16, 2024. The copyright holder for this preprint (which was not certified by peer review) is the author/funder, who has granted bioRxiv a license to display the preprint in perpetuity. It is made available under aCC-BY-NC-ND 4.0 International license.

log(k) values for the ITC task performed seven weeks later (at the end of the dietary intervention); (2) the urgency trait subscale of the Impulsive Behavior Short Scale–8 (I-8). Since we had directional hypotheses, we used one-tailed correlation tests for all correlations between predicted and observed log(k).

Predictions of the brain pattern in an independent sample of healthy participants in Study 2

To assess the predictions of the brain classifier developed in Study 1 in participants of Study 2, we calculated the dot product between the predictive weight map and the grey matter density map of each participant of Study 2. The dot product (computed as a linear combination of the participant's voxel grey matter density multiplied by voxel weight across the brain), plus the classifier's intercept, provides a pattern response and thereby a predicted value of log(k) for each participant. This allowed us to test the correlations between the predicted log(k) values and: (1) the actual log(k) values computed in the sample; (2) the average of positive and negative urgency measures from the UPPS-P Impulsive Behavior Scale.

Predictions of the brain pattern in patients with neurodegenerative dementia in Study 3

To assess the predictions of the brain classifier developed in Study 1 in participants of Study 3, we calculated again the dot product as a measure of pattern response and thereby a predicted value of log(k) for each participant of Study 3. This allowed us to test: (1) the correlation between the predicted log(k) and the actual log(k) values (for both monetary and food rewards) across the whole sample (bvFTD patients and matched controls); (2) whether predicted log(k) values could accurately discriminate between bvFTD patients and controls, using a single-interval test (thresholded for optimal overall accuracy). Further, we explored whether the predicted log(k)'s were related to the severity of inhibition deficit (measured by Hayling error score) and of dysexecutive syndrome (i.e., lower FAB total score) among bvFTD patients.

Bootstrapping and thresholding of the predictive brain pattern obtained in Study 1

We used a bootstrapping analysis to detect the brain regions that were the most robust contributors to predict log(k). Sampling with replacement from the initial sample of Study 1 participants generated 5,000 samples. The LASSO-PCR algorithm yielded a predictive brain pattern (voxel weights across

bioRxiv preprint doi: https://doi.org/10.1101/2024.09.12.612706; this version posted September 16, 2024. The copyright holder for this preprint (which was not certified by peer review) is the author/funder, who has granted bioRxiv a license to display the preprint in perpetuity. It is made available under aCC-BY-NC-ND 4.0 International license.

391 the brain) from the data (paired GMD map – log(k) outcome) in each of these 5,000 samples. For each
392 voxel weight in the whole-brain pattern, the probability of being different from 0 (either above or below
393 0) could be estimated across the 5,000 samples. Thus, two-tailed, uncorrected p-values were
394 calculated for each voxel across the whole brain and false discovery rate (FDR) correction was used
395 to correct for multiple comparisons. Bootstrapped weights were thresholded at q=0.05 FDR-corrected
396 across the whole weight map, as well as at p=0.05 uncorrected for display.
397
398 *Spatial distribution of weights in the predictive brain pattern obtained in Study 1*
399 To further characterize the spatial distribution of regions predicting log(k) and their link to different
400 functional networks, we investigated the similarity between the predictive brain pattern (resulting from
401 the LASSO-PCR procedure) and term-based meta-analytic images [47] representing functional networks
402 that have been previously hypothesized [48] to contribute to temporal discounting, namely brain areas
403 related to valuation, executive control and memory/prospection. We calculated the spatial correlation
404 coefficients (Pearson's r) between the brain pattern (map of weights) and each of the meta-analytic
405 maps (thresholded meta-analytic uniformity maps from Neurosynth) corresponding to the following list
406 of terms: "value", "reward", "emotion", "affect", "executive", "conflict", "cognitive control", "attention",
407 "planning", "imagery", "memory", "episodic memory". These spatial correlations provide descriptive
408 insight into the importance of the contribution of GMD within specific functional networks to predict
409 individual differences in delay discounting [14,49].
410
411 **RESULTS**
412
413 **Development and cross-validation of a structural brain signature predicting delay discounting**
414 **in healthy adults (Study 1)**
415
416 *Individual differences in impulsivity*
417 On average, participants had a fitted log(k) parameter of -5.94 (median log(k)=-5.49, corresponding to
418 k=0.0041). Discounting rates were characterized by substantial individual differences (SD=2.00), with
419 log(k) ranging from -11.92 to -2.16. These individual differences were very stable over a 7-week period
420 as reported previously [14]. On the I-8 subscale of urgency trait, participants' average scores varied

bioRxiv preprint doi: https://doi.org/10.1101/2024.09.12.612706; this version posted September 16, 2024. The copyright holder for this preprint (which was not certified by peer review) is the author/funder, who has granted bioRxiv a license to display the preprint in perpetuity. It is made available under aCC-BY-NC-ND 4.0 International license.

between 1 and 5 (mean=2.72; median=2.5; SD=0.84). Log(k) showed a trend for a weak positive correlation with the urgency trait (R=0.17, p=0.06, 95%-CI= [-0.009, 0.35]).

Cross-validated predictions of delay discounting - Validity of predicted log(k) in healthy participants

The 10-fold cross-validation procedure revealed a significant accuracy of the brain-based prediction (see Figure 2A and 2B and Supplementary figure 1): the predictions had a mean squared error of 3.45 (permutation test: p=0.0026), a root mean squared error of 1.86 (permutation test: p=0.0026), a mean absolute error for predicted log(k) of 1.46 (permutation test: p=0.0022), and a cross-validated prediction-outcome correlation of R=0.35 (permutation test: p=0.0028) (Figure 2C).

Further, supporting the reliability and conceptual validity of the brain-predicted log(k)'s, we found that brain-based predictions at baseline significantly correlated with (out-of-sample) log(k)'s computed from the ITC task performed seven weeks later (R=0.34, p<0.001, 95%-CI= [0.18, 1]) (Figure 2D). This suggests that a relatively stable part of the between-person variability in delay discounting was explained by individual differences in brain structure. Moreover, higher brain-predicted log(k) values were associated with higher self-reported urgency (R=0.20, p=0.037, 95%-CI= [0.01, 0.37]) (Figure 2E).

Like the actual measures of log(k) (see [14]), brain-based predictions of log(k) did not significantly correlate with age (R=-0.11, p=0.24, 95%-CI= [-0.29, 0.07]), education (R=-0.15, p=0.10, 95%-CI= [-0.33, 0.03]), income (R=-0.12, p=0.21, 95%-CI= [-0.30, 0.07]), BMI (R= -0.04, p=0.66, 95%-CI= [-0.22, 0.14]), and percentage of body fat (R= -0.13, p=0.18, 95%-CI= [-0.31, 0.06]) (see more details in Supplementary figure 2).

Performance of the Structural Impulsivity Signature in a second independent sample of healthy participants (Study 2)

Study 2 tests the predictions of the Structural Impulsivity Signature (SIS) in a second MRI dataset of healthy participants, that has used a different protocol, scanner, different preprocessing pipeline, in a socio-demographically different participant population.

Individual differences in impulsivity

bioRxiv preprint doi: https://doi.org/10.1101/2024.09.12.612706; this version posted September 16, 2024. The copyright holder for this preprint (which was not certified by peer review) is the author/funder, who has granted bioRxiv a license to display the preprint in perpetuity. It is made available under aCC-BY-NC-ND 4.0 International license.

The mean log(k) parameter in Study 2 was -4.09 (median log(k)=-3.94, corresponding to a k of 0.019). Individual differences in the discounting parameter were less variable (SD=0.98) as compared to Study 1, with log(k) ranging from -7.08 to -2.12. Participants had average urgency trait scores (means of positive and negative urgency) varying between 1.00 and 3.01 (mean=1.76; median=1.68; SD=0.48). In Study 2, log(k) had a trend for a negative correlation with urgency (R=-0.14, p=0.06, 95%-CI= [-0.29, 0.008]). Therefore, in Study 2, the discounting rate does not seem to be related to individual differences in impulsivity.

Brain-based predictions of impulsivity - Validity of predicted log(k) in a second independent sample of healthy participants

For each participant in Study 2, we calculated the predicted individual log(k) as the dot-product between the weight map developed in Study 1 and the individual GMD map. We then tested whether predicted log(k) correlated with observed individual log(k) and with the impulsivity trait of urgency (UPPS subscales). While we did not find a significant link between predicted and observed log(k) in Study 2 (R=0.06, p=0.21, 95%-CI= [-0.07, 1]), predicted log(k) was positively associated with urgency scales (R=0.15, p=0.047, 95%-CI= [0.002, 0.30], see Figure 2F), as in Study 1. Thus, the results of Study 2 partially validate the developed structural brain signature as a brain signature of impulsivity.

bioRxiv preprint doi: https://doi.org/10.1101/2024.09.12.612706; this version posted September 16, 2024. The copyright holder for this preprint (which was not certified by peer review) is the author/funder, who has granted bioRxiv a license to display the preprint in perpetuity. It is made available under aCC-BY-NC-ND 4.0 International license.

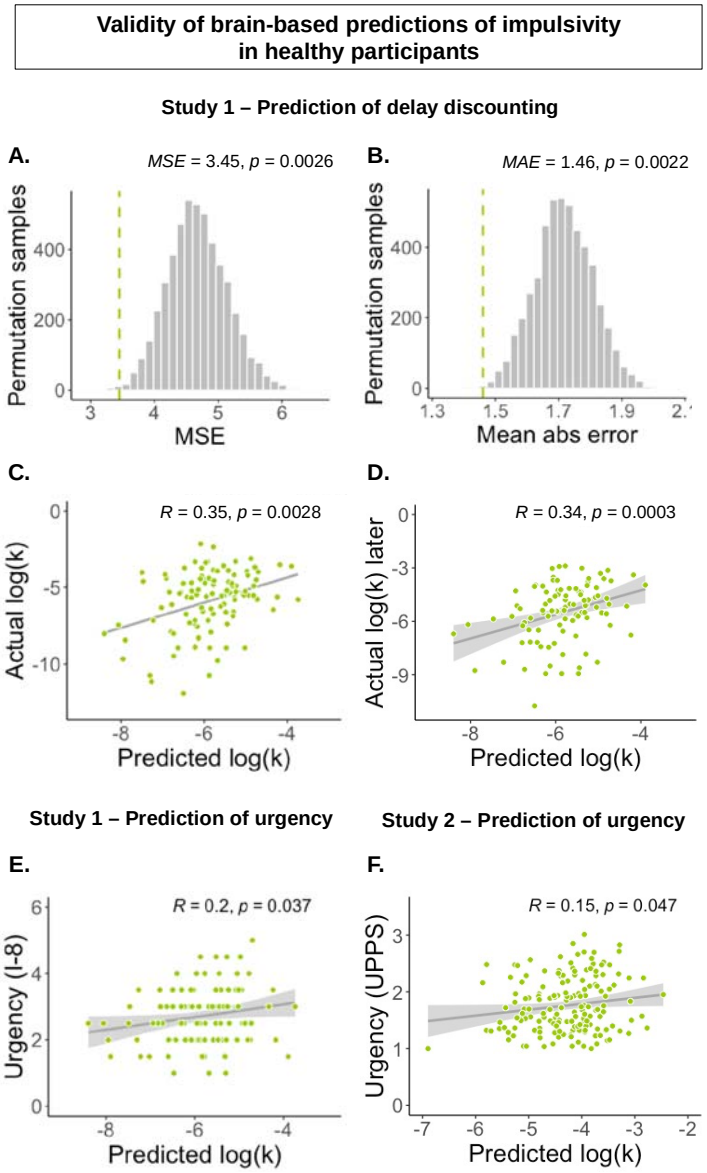

Figure 2. Predictive validity of the structural brain pattern in Study 1 and Study 2. A) Mean squared error (MSE) of prediction and significance obtained by permutation test (5,000 samples – N=113 males). **B)** Mean absolute error (MAE) of prediction and significance obtained by permutation test (5,000 samples – N=113 males). **C)** Correlation between predicted log(k) and actual log(k) in Study 1 and significance of prediction-outcome correlation obtained by permutation test (5,000 samples – N=113 males). **D)** Test of the parametric correlation between predicted log(k) and actual log(k) assessed 7 weeks later in Study 1 (R=0.34, p<0.001, 95%-CI= [0.15, 0.50]). **E)** Test of the parametric correlation between predicted log(k) and self-reported urgency (subscale of I-8 Impulsive Behavior Short Scale) in Study 1 (R=0.20, p=0.037, 95%-CI= [0.01, 0.37]). **F)** Test of the parametric correlation between predicted log(k) and self-reported urgency (mean of positive and negative urgency subscales of UPPS-P Impulsive Behavior Scale) in Study 2 (R=0.15, p=0.047, 95%-CI= [0.002, 0.30]).

bioRxiv preprint doi: https://doi.org/10.1101/2024.09.12.612706; this version posted September 16, 2024. The copyright holder for this preprint (which was not certified by peer review) is the author/funder, who has granted bioRxiv a license to display the preprint in perpetuity. It is made available under aCC-BY-NC-ND 4.0 International license.

Validation of the structural brain signature in a clinical sample of bvFTD patients and matched controls (Study 3)

Our last analysis step aimed at further testing the generalizability of the SIS by evaluating its validity in a patient population that is characterized by impulsivity. Study 3 employed a distinct protocol from Studies 1 and 2 (different ITC task, different MRI scanner and parameters), and in a different, older population including dementia patients with substantial structural atrophy. This further allowed us to investigate the clinical relevance of the SIS (1) for classifying patients with bvFTD differently from matched control participants and (2) for predicting the core symptoms of disinhibition and executive deficits in patients with bvFTD [8] .

Differences of impulsivity between bvFTD patients and healthy controls

In line with the core symptoms of this disorder, bvFTD patients presented significantly higher delay discounting (i.e. more impatient or impulsive choices) compared to controls, for both money rewards and food rewards (see [35]). They also showed higher inhibition deficit (Hayling-error score; t=5.71, p<0.001, Cohen's d=1.60, 95%-CI=[0.87, 2.33]) and lower executive performances (FAB score; t=-7.31, p<0.001, Cohen's d=-2.00, 95%-CI=[-1.23, -2.77]) compared to controls (see Supplementary table 1).

Brain-based predictions of impulsivity – Validity of predicted log(k) in bvFTD patients

To investigate the predictive validity of our classifier in Study 3, we first tested whether predicted log(k)'s (obtained from the brain pattern applied to each participant's grey matter density map) were correlated with actual log(k)'s calculated in this study across the whole sample (patients and controls). This analysis showed that the predicted log(k) values were positively correlated with actual log(k) values, for both monetary rewards (R=0.30, p=0.03, 95%-CI= [0.03, 1], mean absolute error of 2.08) and for food rewards (R=0.40, p=0.006, 95%-CI= [0.15, 1], mean absolute error of 2.65) (see Figure 3.A and 3.B).

We next tested whether the SIS predictions could distinguish bvFTD patients from controls. As expected, we found that brain-predicted log(k) was significantly higher in bvFTD patients than in controls (t=3.60, p= 0.0009, Cohen's d=1.09, 95%-CI=[0.41, 1.76] – see Figure 3.C). Notably, brain-

bioRxiv preprint doi: https://doi.org/10.1101/2024.09.12.612706; this version posted September 16, 2024. The copyright holder for this preprint (which was not certified by peer review) is the author/funder, who has granted bioRxiv a license to display the preprint in perpetuity. It is made available under aCC-BY-NC-ND 4.0 International license.

predicted log(k) significantly predicted whether a grey matter density map was from a bvFTD patient or from a control participant, with a classification accuracy of 81 % (p= 0.002, sensitivity = 87.5%, specificity = 72.2%, - see Figure 3.D). Interestingly, the actual log(k)'s calculated for monetary and food rewards in this sample revealed slightly lower predictive accuracies and especially lower specificities: 73.7 % accuracy for monetary rewards (p= 0.07, sensitivity = 100%, specificity = 37.5%,) and 76.3 % for food rewards (p= 0.01, sensitivity = 100%, specificity = 47.1%).

We next investigated the relationship between brain-predicted log(k) and clinical measures of bvFTD core symptoms of disinhibition and executive deficits. Across both the patient and control groups, higher predicted log(k) was associated with higher inhibition deficit (higher Hayling-error score; R=0.55, p=0.0002, 95%-CI= [0.30, 0.74]) and higher executive troubles (lower FAB score; R=-0.56, p=0.0001, 95%-CI= [-0.74, -0.30]). More interestingly, even within the group of bvFTD patients, higher predicted log(k) was associated with higher inhibition deficit (higher Hayling-error score; R=0.52, p=0.01, 95%-CI= [0.14, 0.77]) and higher executive troubles (lower FAB score; R=-0.43, p=0.04, 95%-CI= [-0.71, -0.03]) (see Figure 3.E and 3.F). Further, we checked that predicted log(k) was still significantly related to lack of inhibition (i.e., higher Hayling-error scores; B=8.63, p=0.02, 95%-CI= [1.51, 15.7]) within bvFTD patients even after controlling for executive function deficit; this added result showed that the relationship between brain-based predictions and disinhibition symptom was not only due to shared variance with the severity of dysexecutive syndrome. Together, these findings show that the SIS significantly and accurately classified bvFTD patients from matched controls, and that it tracked the severity of key symptoms in these patients.

bioRxiv preprint doi: https://doi.org/10.1101/2024.09.12.612706; this version posted September 16, 2024. The copyright holder for this preprint (which was not certified by peer review) is the author/funder, who has granted bioRxiv a license to display the preprint in perpetuity. It is made available under aCC-BY-NC-ND 4.0 International license.

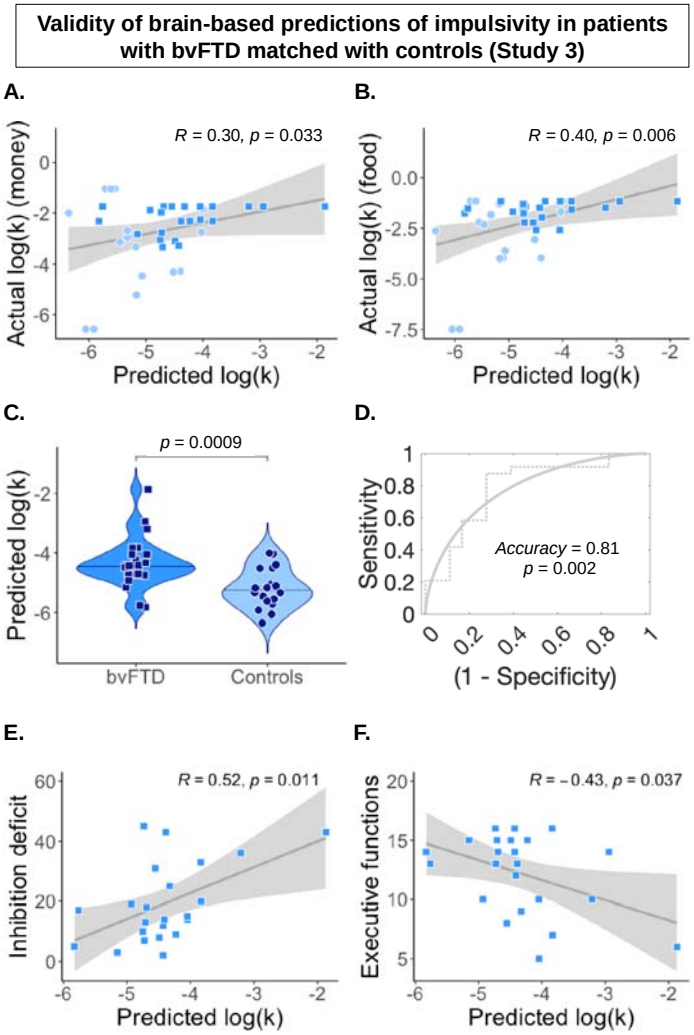

Figure 3. Predictive validity of the structural brain pattern in Study 3. (A) Parametric correlation between predicted log(k) and actual log(k) assessed with monetary rewards in Study 3 (R=0.30, p=0.07, 95%-CI= [-0.02, 0.57]). Patients are represented as squares in darker blue and controls as circles in lighter blue. (**B)** Parametric correlation between predicted log(k) and actual log(k) assessed with food rewards in Study 3 (R=0.45, p=0.01, 95%-CI= [0.1, 0.64]). Patients are represented as squares in darker blue and controls as circles in lighter blue. (**C)** As expected, predicted log(k) was higher in bvFTD patients (N=24) than in controls (N=18) (t=3.60, p=0.0009, Cohen's d=1.09, 95%-CI=[0.41, 1.76]). (**D)** ROC curve showing the performance of the brain-based prediction of log(k) in classification of bvFTD patients versus healthy controls (single interval test thresholded for optimal accuracy: accuracy=81 %, p= 0.002, AUC = 0.80, sensitivity = 87.5%, specificity = 72.2%). (**E)** Higher predicted log(k) was related to greater inhibition deficits (Hayling-error score) in bvFTD patients (R=0.52, p=0.01, 95%-CI= [0.14, 0.77]). (**F)** Higher predicted log(k) was related to more impaired executive functions (as measured with the FAB score) in bvFTD patients (R=-0.43, p=0.04, 95%-CI= [-0.71, -0.03]).

bioRxiv preprint doi: https://doi.org/10.1101/2024.09.12.612706; this version posted September 16, 2024. The copyright holder for this preprint (which was not certified by peer review) is the author/funder, who has granted bioRxiv a license to display the preprint in perpetuity. It is made available under aCC-BY-NC-ND 4.0 International license.

548

549 **Spatial distribution of weights in the structural brain signature (Study 1)**

550

551 *Thresholded pattern of structural brain signature*

552 Bootstrapping results revealed the positive and negative weights that most strongly contributed to
553 GMD-based prediction of individual differences in delay discounting. At a threshold of q=0.05 FDR-
554 corrected, we found two clusters in which grey matter density positively contributed to discounting
555 differences (which means that higher grey matter density was associated with higher impatience);
556 these clusters were in the left lateral parietal cortex (supramarginal gyrus) and left lateral occipital
557 cortex (superior division). At a threshold of p=0.001 uncorrected, we found additional clusters
558 contributing positive weights, especially in regions of the valuation system [50] such as the right
559 orbitofrontal cortex (OFC), ventromedial prefrontal cortex (vmPFC) and right ventral striatum.
560 At q=0.05 FDR-corrected, there was one cluster in the posterior cingulate cortex (PCC) and adjacent
561 lingual gyrus (including retrosplenial cortex) in which grey matter density contributed negatively to
562 discounting differences (i.e., in which lower grey matter density was associated with higher
563 impatience). At a threshold of p=0.001 uncorrected, other important regions contributing negative
564 weights were found in the left hippocampus, the right anterior insulae (AI), dorsal anterior cingulate
565 cortex (ACC), and amygdalae. For display purposes, the bootstrapped weight map is displayed in
566 Figure 3A at a more comprehensive threshold (p=0.05 uncorrected, see also Supplementary table 2).

567

568 *Similarity of structural brain signature to meta-analytic maps*

569 When comparing the predictive map of log(k) with meta-analytic uniformity maps [47], we observed that
570 the highest similarities (spatial correlation r's > 0.1 in absolute value) were with the "Emotions",
571 "Affect", "Conflict" and "Imagery" meta-analytic maps (Figure 4B). These spatial correlations were all
572 negative, indicating that greater grey matter density in areas related to emotions, affect, conflict
573 processing, and imagery contributes to predicting lower delay discounting or more 'patient' decision-
574 making (or conversely, lower grey matter density in these areas predicts higher discounting and more
575 impulsive decision-making). The "Emotions", "Affect", "Conflict" and "Imagery" meta-analytic maps
576 correspond to overlapping functional networks (see Figure 4.B). Among the most overlapping regions
577 between these four networks (in red), the AI and dorsal ACC, corresponding to robust negative
578 weights in the brain pattern, are known to be major hubs of the salience network [51].

bioRxiv preprint doi: https://doi.org/10.1101/2024.09.12.612706; this version posted September 16, 2024. The copyright holder for this preprint (which was not certified by peer review) is the author/funder, who has granted bioRxiv a license to display the preprint in perpetuity. It is made available under aCC-BY-NC-ND 4.0 International license.

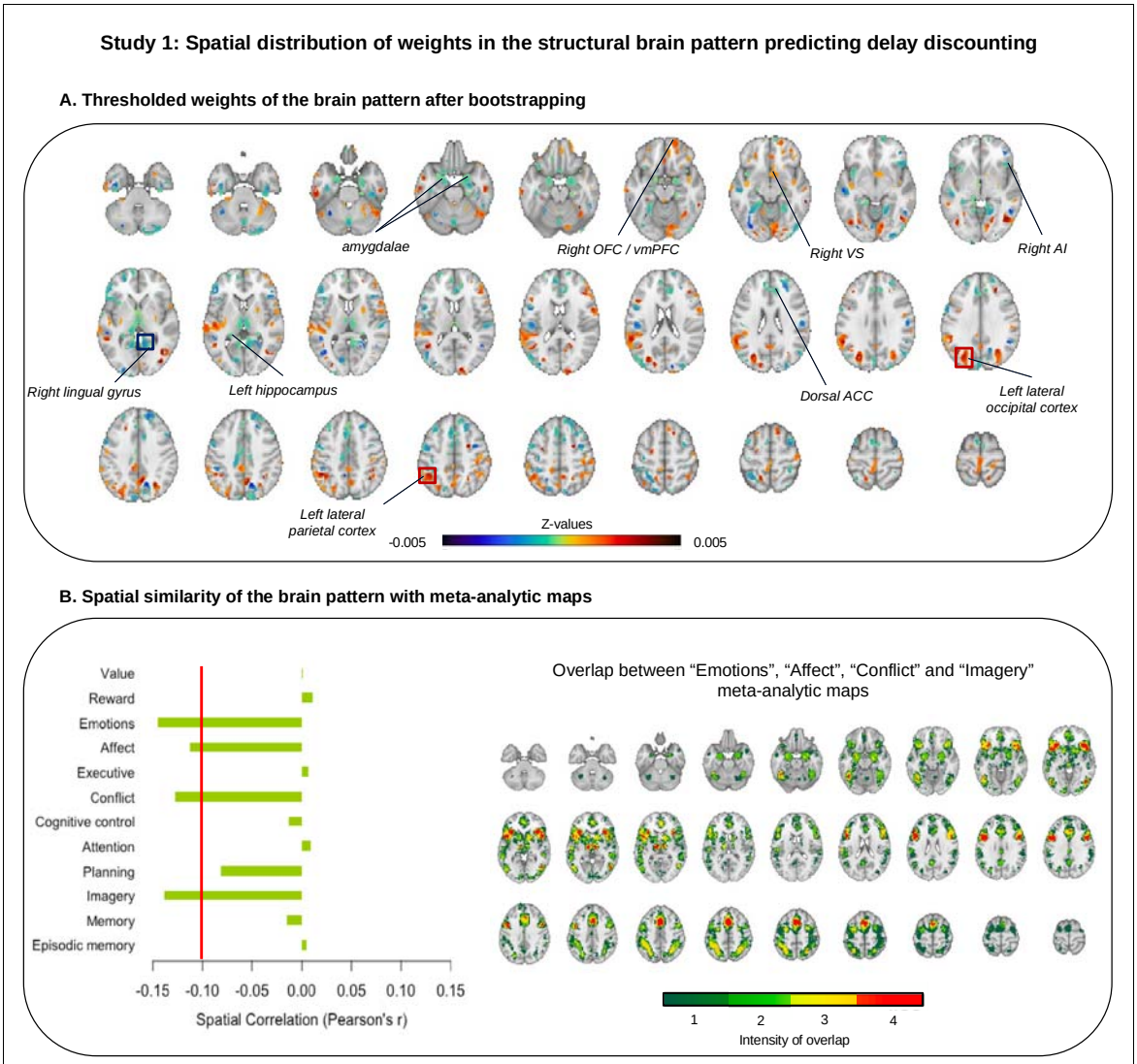

Figure 4. Spatial organization of the structural brain pattern developed in Study 1. A) Whole-brain weight map thresholded at p=0.05 (uncorrected for multiple comparisons across the brain) resulting from a bootstrapping procedure (5,000 samples); negative weights (contributing to lower discounting with higher grey matter density) are shown in blue. Positive weights (contributing to higher discounting with higher grey matter density) are shown in orange. The three framed clusters correspond to the three clusters in which peaks are significant at q=0.05 FDR-corrected. Regions indicated in italics are some of the main regions significant at p=0.001, uncorrected (OFC: orbitofrontal cortex; vmPFC: ventromedial prefrontal cortex; VS: ventral striatum; AI: anterior insula; ACC: anterior cingulate cortex). **B)** On the left, spatial correlations of the unthresholded delay discounting brain pattern with thresholded meta-analytic uniformity maps from Neurosynth (http://www.neurosynth.org). As in [14], we selected meta-analytic maps corresponding to three types of functions assumed to be involved in delay discounting: 1/ valuation and emotion processing; 2/ executive control; 3/ memory and prospection. Spatial correlations are descriptive and indicate the extent of spatial similarities between the structural brain pattern and the functional networks of interest [47]. Highest correlations (or

bioRxiv preprint doi: https://doi.org/10.1101/2024.09.12.612706; this version posted September 16, 2024. The copyright holder for this preprint (which was not certified by peer review) is the author/funder, who has granted bioRxiv a license to display the preprint in perpetuity. It is made available under aCC-BY-NC-ND 4.0 International license.

similarities) were observed with the “Emotions”, “Affect”, “Conflict”, and “Imagery” meta-analytic maps, and were all negative, meaning that higher grey matter density in these functional regions is associated with lower discounting. On the right, we show the spatial distribution and overlap between the four meta-analytic maps found to be the most negatively correlated with the structural brain pattern (from 1, corresponding to non-overlapping regions from only one map, to 4, corresponding to regions of overlap between the 4 maps).

Spatial distribution of brain regions contributing to higher predicted log(k) in bvFTD (Study 3)

To identify the main brain regions which contributed to differentiate bvFTD patients from controls on the brain-predicted log(k), we contrasted bvFTD patients versus controls in terms of voxel-wise pattern expression of the predictive map of log(k). To this end, for each bvFTD patient and each control participant, we computed an ‘importance map’ as the unsummed matrix dot product between the predictive structural weight map and the individual grey matter density map. Since higher resulting dot product contributes to higher predicted discounting, the importance map shows which brain regions contributed to increase (or decrease) predicted discounting in each individual. We performed a t-test contrasting bvFTD patients and controls (bvFTD > controls) on the resulting importance maps, with a family-wise error (FWE) correction applied to p-values to correct for multiple comparisons across the brain (see Figure 5.C). This contrast shows the regions in which structural atrophy contributed positively to higher predicted discounting in bvFTD than in controls (regions in red). These included the OFC, anterior insulae, dorsal ACC, striatum, thalamus, amygdalae, hippocampus, and middle temporal regions. These regions corresponded to areas combining the presence of negative weights in the predictive brain pattern (i.e., voxels for which higher GMD predicts lower discounting and more patient decision-making, shown in Figure 5.B) and the presence of significant grey matter atrophy due to bvFTD pathology (see atrophy pattern in Figure 5.A). Thus, the contrast shown in Figure 5.C also maps the regions in which the SIS is the most similar to bvFTD atrophy pattern.

bioRxiv preprint doi: https://doi.org/10.1101/2024.09.12.612706; this version posted September 16, 2024. The copyright holder for this preprint (which was not certified by peer review) is the author/funder, who has granted bioRxiv a license to display the preprint in perpetuity. It is made available under aCC-BY-NC-ND 4.0 International license.

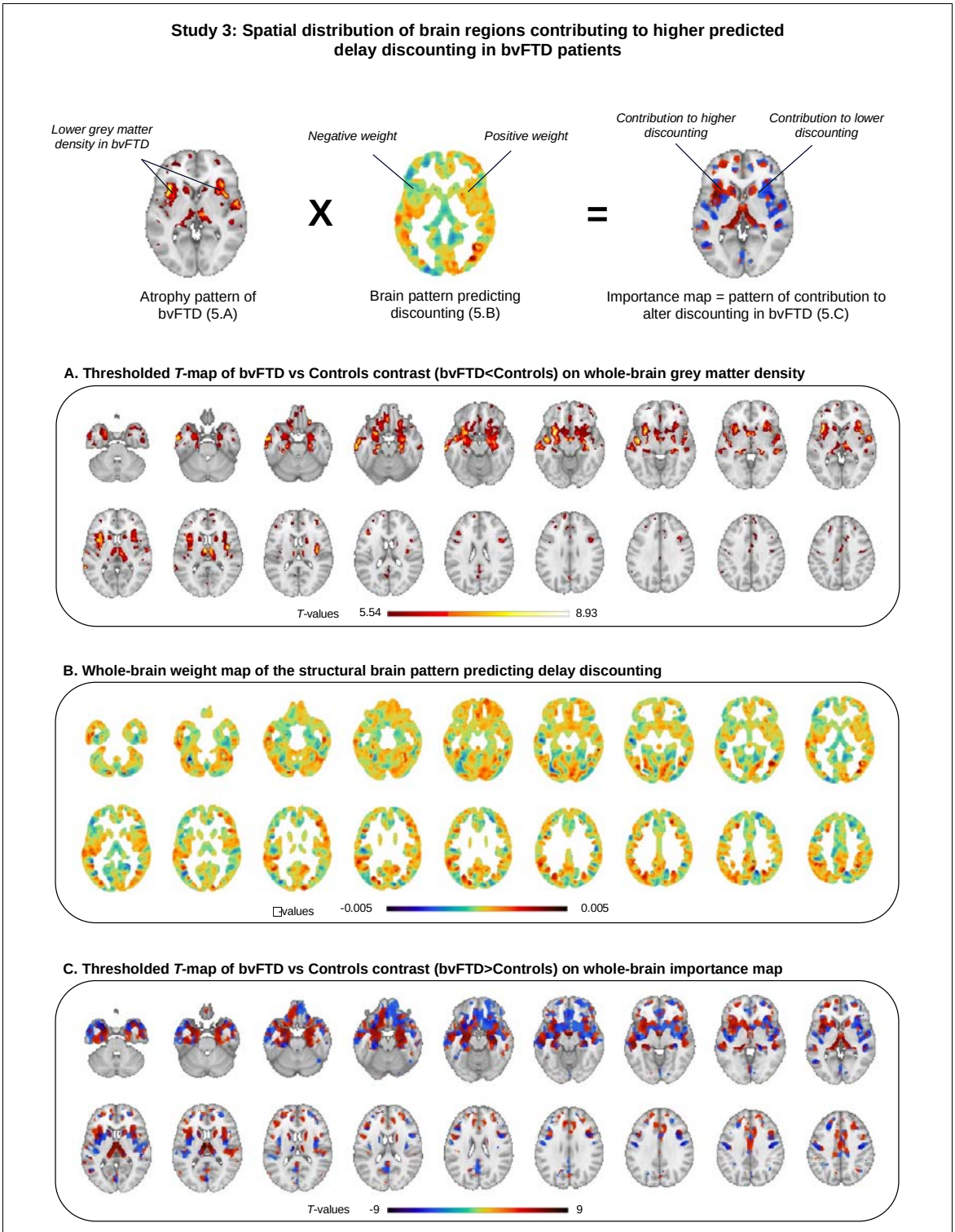

Figure 5. Spatial distribution of regions contributing to higher predicted discounting in bvFTD in Study 3. We computed an importance map as the unsummed matrix dot product between the Structural Impulsivity Signature (SIS) (developed in Study 1) and the individual grey matter density map of each Study 3 participant. Since higher resulting dot product contributes to higher predicted

bioRxiv preprint doi: https://doi.org/10.1101/2024.09.12.612706; this version posted September 16, 2024. The copyright holder for this preprint (which was not certified by peer review) is the author/funder, who has granted bioRxiv a license to display the preprint in perpetuity. It is made available under aCC-BY-NC-ND 4.0 International license.

discounting, the importance map shows how brain regions contribute to increased (or decreased) predicted discounting in each individual. We performed a t-test contrasting bvFTD patients and controls (bvFTD > controls) on the resulting importance maps, to show in particular the regions in which the contribution to higher discounting was significantly higher in bvFTD than in controls. Within regions showing atrophy in bvFTD (see 6.A), those corresponding to negative (/positive) weights in the whole-brain predictive pattern (see 6.B) contributed to increase (/decrease) discounting in bvFTD (see 6.C). (**A)** VBM–derived grey matter atrophy map of bvFTD patients contrasted with matched controls (bvFTD<Controls), FWE-corrected and thresholded at $p < 0.05$. (**B)** Unthresholded whole-brain weight map of the structural brain pattern developed in Study 1 and used in Study 2 to predict delay discounting in bvFTD patients (N=24) and matched controls (N=18). Negative weights (contributing to lower discounting with higher grey matter density) are in blue and positive weights (contributing to higher discounting with higher grey matter density) are in orange. (**C)** Contrast between bvFTD patients and controls (bvFTD>Controls)) on the importance map, FWE-corrected and thresholded at $p < 0.05$; this map shows regions contributing to increase discounting in bvFTD patients (compared to controls) in red and regions contributing to decrease discounting in bvFTD patients (compared to controls) in blue, the balance being in favor of a global increase in predicted discounting in bvFTD patients.

bioRxiv preprint doi: https://doi.org/10.1101/2024.09.12.612706; this version posted September 16, 2024. The copyright holder for this preprint (which was not certified by peer review) is the author/funder, who has granted bioRxiv a license to display the preprint in perpetuity. It is made available under aCC-BY-NC-ND 4.0 International license.

DISCUSSION

Impulsive and maladaptive decision-making is a transversal feature of many mental disorders, especially prominent in behavioral-variant frontotemporal dementia (bvFTD). Yet, its relationship with individual brain characteristics, in particular brain structure, is still debated. Here, we used a machine learning technique to develop a brain signature (i.e., a multi-variate brain model) of individual differences in delay discounting—a facet of impulsivity—based on whole-brain grey matter density patterns. We performed out-of-sample cross-validation in a first sample of 117 healthy adults (Study 1) used for brain signature development. We further tested the generalizability of this brain signature developed in Study 1 in two independent studies: a second sample of 166 healthy adults (Study 2) and a clinical study including 24 bvFTD patients and 18 matched controls (Study 3). Individual differences of whole-brain grey matter density reliably predicted individual differences in discounting rates in the first sample of healthy adults but not in the second independent sample. However, the brain signature predicted individual differences of urgency (a subcomponent of impulsivity according to the UPPS model) with small-to-moderate effect sizes in both the first and the second samples of healthy adults. Most importantly, in the clinical study, we found that this structural signature of impulsivity (SIS) separated bvFTD patients from controls with 81% accuracy and that it significantly predicted not only individual differences in delay discounting across participants but also inhibition deficit (objectively assessed from the Hayling test), even within the group of bvFTD patients. Thus, the SIS might be more closely and reliably related to the broader concepts of impulsivity, urgency, and inhibition deficits rather than to specifically delay discounting, which may be more driven by cultural and educational factors than trait urgency. In sum, our results suggest that: 1) it is possible to predict individual differences in impulsivity from whole-brain structure and 2) this novel brain signature is sensitive to the structural atrophy that is characteristic of bvFTD, making it a novel candidate neuromarker for improving bvFTD diagnosis.

The identification of the SIS advances our knowledge of the neurobiology underlying individual differences in impulsivity. Higher discounting (i.e., greater impulsivity) was associated with higher grey matter density in clusters of the lateral parietal and occipital cortex as well as in regions of the OFC, vmPFC, ventral striatum, lateral PFC, precentral gyrus, and precuneus. Functional activation of these regions during intertemporal choices and in response to rewards has previously been shown to predict

bioRxiv preprint doi: https://doi.org/10.1101/2024.09.12.612706; this version posted September 16, 2024. The copyright holder for this preprint (which was not certified by peer review) is the author/funder, who has granted bioRxiv a license to display the preprint in perpetuity. It is made available under aCC-BY-NC-ND 4.0 International license.

675 higher discounting [14,52]. The SIS obtained from Study 1 also revealed regions in which greater grey
676 matter density contributes to lower individual impulsivity. Among the strongest negative contributors,
677 we found clusters corresponding to hub regions of the salience network (anterior insulae, dorsal ACC,
678 amygdalae). Dorsal ACC and anterior insula were also consistently found as significant regions
679 predicting delay discounting from whole-brain functional MRI [14]. These regions are associated with the
680 processing of emotionally significant internal and external stimuli [51,53,54] and awareness of present and
681 future affective states [55]; they are also supposed to be involved in switching between large-scale
682 networks to facilitate access to attention and working memory resources in the presence of a salient
683 event [56]. These areas are also known to be involved in cognitive conflict processing [57,58] and previous
684 studies have shown their response to difficult choices (characterized by choice conflicts between
685 options) during delay discounting [59]. Thus, our results suggest that more impulsive individuals might
686 be those for whom lower affective, attentional, and conflict processing would lead to more impulsive
687 decision-making, favouring immediately rewarding options over long-term consequences of behavior.
688 The SIS has the potential to contribute to the early diagnosis of conditions characterized by
689 high impulsivity, such as bvFTD. Brain signatures can in particular help the diagnosis of conditions
690 involving brain lesions that are sometimes difficult to detect by mere visual inspection of MRI scans,
691 especially at early stages of the disease. In addition, brain signatures can constitute neuroimaging
692 markers with diagnostic value that can be used across different samples and populations [11,60]. The SIS
693 may contribute to the diagnosis of bvFTD by complementing other brain models able to detect bvFTD.
694 A few previous studies successfully trained structural MRI classifiers for the specific purpose of
695 distinguishing FTD patients from controls (e.g., [61–63]). These bvFTD classifiers have shown their
696 accuracy to detect patients with clear structural brain damage but their ability to distinguish individuals
697 at risk of developing FTD due to genetic mutations is likely to be limited to the period just before
698 symptom onset [64,65]. Under the hypothesis of a continuum of marked impulsivity in presymptomatic
699 individuals and patients [16], the SIS might serve the early prediction and monitoring of bvFTD before
700 symptom onset. Impulsive behaviors may be present in an attenuated form long before clinical
701 diagnosis and hard to detect with traditional clinical methods. A neuromarker predicting impulsivity
702 may be sensitive to specific brain modifications that appear very early in individuals predisposed to
703 FTD (possibly as neurodevelopmental lesions [66]) and would thus allow to enhance the monitoring of

bioRxiv preprint doi: https://doi.org/10.1101/2024.09.12.612706; this version posted September 16, 2024. The copyright holder for this preprint (which was not certified by peer review) is the author/funder, who has granted bioRxiv a license to display the preprint in perpetuity. It is made available under aCC-BY-NC-ND 4.0 International license.

clinical signs of these subtle behavioral changes. Future tests of this brain signature in presymptomatic populations will allow to evaluate these potential clinical applications.

As it predicts nearly 30% of the variance of inhibition deficit among bvFTD patients, the SIS may be sensitive to lesions in a structural network underlying the core bvFTD symptom of disinhibition. In addition to its potential contribution to the early detection of presymptomatic individuals, this brain signature may thus aid differential diagnosis and provide insight into the neuropsychological profiles of patients. The SIS may for instance help to distinguish bvFTD from other neurodegenerative or neuropsychiatric conditions with different core symptoms. The differential diagnosis of Alzheimer's disease and bvFTD can in particular be challenging. Using neuromarkers such as the SIS in cases of diagnostic uncertainty potentially impacting the choice of treatment could therefore be highly valuable [67] and should be an avenue for future studies. Moreover, the SIS could become a useful tool to disentangle the phenotypic heterogeneity within bvFTD population [68]. The characterization of different clinical and behavioral profiles within the bvFTD spectrum could help to better understand the pathology, and to better adapt treatments according to patients' specific needs.

Despite holding promises for future clinical applications, we note that our results also point at challenges in generalizing the brain signature to other independent samples of healthy adults. We were successful at predicting delay discounting from whole-brain grey matter in a first rather homogenous sample of healthy adults (male participants, controlled experimental conditions) showing significant variability in terms of impulsivity and a positive correlation between the discounting rate and urgency. In a second independent sample of healthy adults with lower variance of impulsivity and a slightly negative correlation between the discounting rate and urgency, we could not replicate the association with measured discounting rates but found evidence of the conceptual validity (i.e., a link with the urgency trait) of brain-based predictions. This suggests that the variance captured by the SIS developed in the first sample is more reliably related to individual differences in urgency than to individual differences in discounting. The fact that urgency was slightly negatively correlated with the discounting rate in the second healthy sample questions the idea that delay discounting necessarily captures individual differences in impulsivity. These two constructs overlap but are not equivalent and previous studies have already reported an absence of link between delay discounting and some psychometric measures of impulsivity (e.g., [69,70]). Discounting rate is also a state-dependent variable [71] and depends on situational factors such as cultural and social context [72]. In addition, the links

bioRxiv preprint doi: https://doi.org/10.1101/2024.09.12.612706; this version posted September 16, 2024. The copyright holder for this preprint (which was not certified by peer review) is the author/funder, who has granted bioRxiv a license to display the preprint in perpetuity. It is made available under aCC-BY-NC-ND 4.0 International license.

734 between personality and discounting rates may depend on participants' cognitive abilities [73].
735 Therefore, association between delay discounting and other measures of trait impulsivity may vary
736 according to samples and studies. A promising approach for future studies would therefore be to
737 predict latent variables that underlie different observed variables related to the same concept of
738 impulsivity (instead of only one observed variable such as the discounting rate), which might achieve
739 better performance in terms of replicability and generalizability [9]. Although multivariate brain
740 signatures can be replicable with moderate sample sizes [74], future studies aiming to develop brain
741 signatures of impulsivity could also benefit from using larger and more diverse samples [75]. More
742 generally, we note that our results suggest a relatively small contribution of interindividual variability in
743 brain structure to interindividual variability in impulsivity among healthy adults. Effect sizes of
744 associations between predicted and observed impulsivity are however in line with those reported for
745 most brain signatures of behavioral individual differences using structural features [9]. Moreover, like
746 variability in brain structure, variability in genotype accounts for a rather small part of the variance of
747 impulsivity [76]. The magnitude of associations between brain structure and behaviors may be limited in
748 the general population but these associations might be more salient within populations with a marked
749 variability of both brain and behavior such as patients with neurodegenerative conditions.

750 In conclusion, our results advance our knowledge of the association between impulsivity and
751 brain structure in healthy adults and in patients with bvFTD. They also point at inherent challenges in
752 developing replicable and generalizable brain signatures of individual differences based on brain
753 structure. By identifying a structural network associated with individual differences in discounting rates,
754 our results provide insight into the potential neurobiological bases of trait impulsivity (and in particular
755 its urgency component). The good performance of the SIS among patients with bvFTD suggests a
756 possible continuum of brain-impulsivity relationship across healthy and clinical conditions. Most
757 noteworthy, the SIS separates bvFTD patients from controls with high accuracy, pointing at the
758 potential clinical value for the diagnosis of bvFTD, in particular for the purpose of stratifying this
759 heterogenous condition. MRI can be instrumental to confirm an FTD diagnosis [67] and the SIS only
760 requires a preprocessed T1-weighted scan to reach a prediction. It holds promise as a phenotypic
761 marker in patients with neurodegenerative or psychiatric conditions associated with high impulsivity.
762 Future studies could test its clinical potential and whether this brain signature could be used in a real-
763 life patient workflow.

bioRxiv preprint doi: https://doi.org/10.1101/2024.09.12.612706; this version posted September 16, 2024. The copyright holder for this preprint (which was not certified by peer review) is the author/funder, who has granted bioRxiv a license to display the preprint in perpetuity. It is made available under aCC-BY-NC-ND 4.0 International license.

764

bioRxiv preprint doi: https://doi.org/10.1101/2024.09.12.612706; this version posted September 16, 2024. The copyright holder for this preprint (which was not certified by peer review) is the author/funder, who has granted bioRxiv a license to display the preprint in perpetuity. It is made available under aCC-BY-NC-ND 4.0 International license.

765 **REFERENCES**

766

767 1. Chamberlain, S. R. & Sahakian, B. J. The neuropsychiatry of impulsivity. *Curr. Opin. Psychiatry*
768 **20**, 255–261 (2007).
769 2. Chamberlain, S. R., Stochl, J., Redden, S. A. & Grant, J. E. Latent traits of impulsivity and
770 compulsivity: toward dimensional psychiatry. *Psychol. Med.* **48**, 810–821 (2018).
771 3. Goodwin, B. C., Browne, M., Hing, N. & Russell, A. M. Applying a revised two-factor model of
772 impulsivity to predict health behaviour and well-being. *Personal. Individ. Differ.* **111**, 250–255
773 (2017).
774 4. Rogers, M. M., Kelley, K. & McKinney, C. Trait impulsivity and health risk behaviors: A latent
775 profile analysis. *Personal. Individ. Differ.* **171**, 110511 (2021).
776 5. Bjork, J. M., Momenan, R. & Hommer, D. W. Delay discounting correlates with proportional lateral
777 frontal cortex volumes. *Biol. Psychiatry* **65**, 710–713 (2009).
778 6. MacNiven, K. H., Leong, J. K. & Knutson, B. Medial forebrain bundle structure is linked to human
779 impulsivity. *Sci. Adv.* **6**, eaba4788 (2020).
780 7. Pehlivanova, M. *et al.* Diminished cortical thickness is associated with impulsive choice in
781 adolescence. *J. Neurosci.* **38**, 2471–2481 (2018).
782 8. Rascovsky, K. *et al.* Sensitivity of revised diagnostic criteria for the behavioural variant of
783 frontotemporal dementia. *Brain* **134**, 2456–2477 (2011).
784 9. Genon, S., Eickhoff, S. B. & Kharabian, S. Linking interindividual variability in brain structure to
785 behaviour. *Nat. Rev. Neurosci.* **23**, 307–318 (2022).
786 10. Kragel, P. A., Koban, L., Barrett, L. F. & Wager, T. D. Representation, Pattern Information, and
787 Brain Signatures: From Neurons to Neuroimaging. *Neuron* **99**, 257–273 (2018).
788 11. Woo, C.-W., Chang, L. J., Lindquist, M. A. & Wager, T. D. Building better biomarkers: brain
789 models in translational neuroimaging. *Nat. Neurosci.* **20**, 365–377 (2017).
790 12. Anokhin, A. P., Grant, J. D., Mulligan, R. C. & Heath, A. C. The Genetics of Impulsivity: Evidence
791 for the Heritability of Delay Discounting. *Biol. Psychiatry* **77**, 887–894 (2015).
792 13. Kirby, K. N. One-year temporal stability of delay-discount rates. *Psychon. Bull. Rev.* **16**, 457–462
793 (2009).
794 14. Koban, L. *et al.* An fMRI-based brain marker of individual differences in delay discounting. *J.*

bioRxiv preprint doi: https://doi.org/10.1101/2024.09.12.612706; this version posted September 16, 2024. The copyright holder for this preprint (which was not certified by peer review) is the author/funder, who has granted bioRxiv a license to display the preprint in perpetuity. It is made available under aCC-BY-NC-ND 4.0 International license.

Neurosci. (2023).

15. Amlung, M. *et al.* Delay Discounting as a Transdiagnostic Process in Psychiatric Disorders: A Meta-analysis. *JAMA Psychiatry* **76**, 1176 (2019).
16. Godefroy, V. *et al.* Altered delay discounting in neurodegeneration: insight into the underlying mechanisms and perspectives for clinical applications. *Neurosci. Biobehav. Rev.* 105048 (2023).
17. Ballard, K. & Knutson, B. Dissociable neural representations of future reward magnitude and delay during temporal discounting. *Neuroimage* **45**, 143–150 (2009).
18. Bergström, F., Lerman, C. & Kable, J. W. Reduced cortical complexity in ventromedial prefrontal cortex is associated with a greater preference for risky and immediate rewards. *Imaging Neurosci.* **2**, 1–14 (2024).
19. Cooper, N., Kable, J. W., Kim, B. K. & Zauberman, G. Brain activity in valuation regions while thinking about the future predicts individual discount rates. *J. Neurosci.* **33**, 13150–13156 (2013).
20. Hare, T. A., Hakimi, S. & Rangel, A. Activity in dlPFC and its effective connectivity to vmPFC are associated with temporal discounting. *Front. Neurosci.* **8**, 50 (2014).
21. Lebreton, M. *et al.* A critical role for the hippocampus in the valuation of imagined outcomes. *PLoS Biol.* **11**, e1001684 (2013).
22. Li, N. *et al.* Resting-State Functional Connectivity Predicts Impulsivity in Economic Decision-Making. *J. Neurosci.* **33**, 4886–4895 (2013).
23. van den Bos, W., Rodriguez, C. A., Schweitzer, J. B. & McClure, S. M. Connectivity strength of dissociable striatal tracts predict individual differences in temporal discounting. *J. Neurosci.* **34**, 10298–10310 (2014).
24. Bartra, O., McGuire, J. T. & Kable, J. W. The valuation system: a coordinate-based meta-analysis of BOLD fMRI experiments examining neural correlates of subjective value. *Neuroimage* **76**, 412–427 (2013).
25. Levy, D. J. & Glimcher, P. W. The root of all value: a neural common currency for choice. *Curr. Opin. Neurobiol.* **22**, 1027–1038 (2012).
26. Rangel, A. & Clithero, J. A. Value normalization in decision making: theory and evidence. *Curr. Opin. Neurobiol.* **22**, 970–981 (2012).
27. Chare, L. *et al.* New criteria for frontotemporal dementia syndromes: clinical and pathological diagnostic implications. *J. Neurol. Neurosurg. Psychiatry* **85**, 865–870 (2014).

bioRxiv preprint doi: https://doi.org/10.1101/2024.09.12.612706; this version posted September 16, 2024. The copyright holder for this preprint (which was not certified by peer review) is the author/funder, who has granted bioRxiv a license to display the preprint in perpetuity. It is made available under aCC-BY-NC-ND 4.0 International license.

28. Karageorgiou, E. & Miller, B. Frontotemporal Lobar Degeneration: A Clinical Approach. *Semin. Neurol.* **34**, 189–201 (2014).
29. Beagle, A. J. *et al.* Amount and delay insensitivity during intertemporal choice in three neurodegenerative diseases reflects dorsomedial prefrontal atrophy. *Cortex J. Devoted Study Nerv. Syst. Behav.* **124**, 54–65 (2020).
30. Bertoux, M., O'Callaghan, C., Flanagan, E., Hodges, J. R. & Hornberger, M. Fronto-striatal atrophy in behavioral variant frontotemporal dementia and Alzheimer's disease. *Front. Neurol.* **6**, 147 (2015).
31. Chiong, W. *et al.* Neuroeconomic dissociation of semantic dementia and behavioural variant frontotemporal dementia. *Brain J. Neurol.* **139**, 578–587 (2016).
32. Manuel, A. L. *et al.* Interactions between decision-making and emotion in behavioral-variant frontotemporal dementia and Alzheimer's disease. *Soc. Cogn. Affect. Neurosci.* **15**, 681–694 (2020).
33. Han, D., Qu, L., Sun, L. & Sun, Y. Variable selection for a mark-specific additive hazards model using the adaptive LASSO. *Stat. Methods Med. Res.* **30**, 2017–2031 (2021).
34. Tibshirani, R. Regression shrinkage and selection via the lasso. *J. R. Stat. Soc. Ser. B Methodol.* **58**, 267–288 (1996).
35. Godefroy, V. *et al.* High delay discounting relates to core symptoms and to pulvinar atrophy in frontotemporal dementia. Preprint at https://doi.org/10.1101/2024.05.16.594526 (2024).
36. Kable, J. W. *et al.* No Effect of Commercial Cognitive Training on Brain Activity, Choice Behavior, or Cognitive Performance. *J. Neurosci.* **37**, 7390–7402 (2017).
37. Groskurth, K., Nießen, D., Rammstedt, B. & Lechner, C. M. The impulsive behavior short scale–8 (I-8): A comprehensive validation of the English-language adaptation. *Plos One* **17**, e0273801 (2022).
38. Whiteside, S. P. & Lynam, D. R. The five factor model and impulsivity: Using a structural model of personality to understand impulsivity. *Personal. Individ. Differ.* **30**, 669–689 (2001).
39. Burgess, P. W. & Shallice, T. The hayling and brixton tests. (1997).
40. Dubois, B., Slachevsky, A., Litvan, I. & Pillon, B. The FAB: a frontal assessment battery at bedside. *Neurology* **55**, 1621–1626 (2000).
41. Flanagan, E. C. *et al.* False recognition in behavioral variant frontotemporal dementia and

bioRxiv preprint doi: https://doi.org/10.1101/2024.09.12.612706; this version posted September 16, 2024. The copyright holder for this preprint (which was not certified by peer review) is the author/funder, who has granted bioRxiv a license to display the preprint in perpetuity. It is made available under aCC-BY-NC-ND 4.0 International license.

Alzheimer's disease—disinhibition or amnesia? *Front. Aging Neurosci.* **8**, 177 (2016).

42. Wileyto, E. P., Audrain-McGovern, J., Epstein, L. H. & Lerman, C. Using logistic regression to estimate delay-discounting functions. *Behav. Res. Methods Instrum. Comput.* **36**, 41–51 (2004).
43. Wager, T. D., Atlas, L. Y., Leotti, L. A. & Rilling, J. K. Predicting Individual Differences in Placebo Analgesia: Contributions of Brain Activity during Anticipation and Pain Experience. *J. Neurosci.* **31**, 439–452 (2011).
44. Wager, T. D. *et al.* An fMRI-Based Neurologic Signature of Physical Pain. *N. Engl. J. Med.* **368**, 1388–1397 (2013).
45. Poldrack, R. A., Huckins, G. & Varoquaux, G. Establishment of best practices for evidence for prediction: a review. *JAMA Psychiatry* **77**, 534–540 (2020).
46. Scheinost, D. *et al.* Ten simple rules for predictive modeling of individual differences in neuroimaging. *NeuroImage* **193**, 35–45 (2019).
47. Yarkoni, T., Poldrack, R. A., Nichols, T. E., Van Essen, D. C. & Wager, T. D. Large-scale automated synthesis of human functional neuroimaging data. *Nat. Methods* **8**, 665–670 (2011).
48. Peters, J. & Büchel, C. The neural mechanisms of inter-temporal decision-making: understanding variability. *Trends Cogn. Sci.* **15**, 227–239 (2011).
49. Koban, L., Jepma, M., López-Solà, M. & Wager, T. D. Different brain networks mediate the effects of social and conditioned expectations on pain. *Nat. Commun.* **10**, 1–13 (2019).
50. Lempert, K. M., Steinglass, J. E., Pinto, A., Kable, J. W. & Simpson, H. B. Can delay discounting deliver on the promise of RDoC? *Psychol. Med.* **49**, 190–199 (2019).
51. Menon, V. Salience Network. in *Brain Mapping* 597–611 (Elsevier, 2015). doi:10.1016/B978-0-12-397025-1.00052-X.
52. Hariri, A. R. *et al.* Preference for immediate over delayed rewards is associated with magnitude of ventral striatal activity. *J. Neurosci.* **26**, 13213–13217 (2006).
53. Seeley, W. W. The salience network: a neural system for perceiving and responding to homeostatic demands. *J. Neurosci.* **39**, 9878–9882 (2019).
54. Seeley, W. W., Zhou, J. & Kim, E.-J. Frontotemporal dementia: what can the behavioral variant teach us about human brain organization? *The Neuroscientist* **18**, 373–385 (2012).
55. Craig, A. D., How do you feel — now? The anterior insula and human awareness. *Nat. Rev. Neurosci.* **10**, 59–70 (2009).

bioRxiv preprint doi: https://doi.org/10.1101/2024.09.12.612706; this version posted September 16, 2024. The copyright holder for this preprint (which was not certified by peer review) is the author/funder, who has granted bioRxiv a license to display the preprint in perpetuity. It is made available under aCC-BY-NC-ND 4.0 International license.

885 56. Menon, V. & Uddin, L. Q. Saliency, switching, attention and control: a network model of insula
886 function. *Brain Struct. Funct.* **214**, 655–667 (2010).
887 57. Botvinick, M. M., Braver, T. S., Barch, D. M., Carter, C. S. & Cohen, J. D. Conflict monitoring and
888 cognitive control. *Psychol. Rev.* **108**, 624 (2001).
889 58. Van Veen, V., Cohen, J. D., Botvinick, M. M., Stenger, V. A. & Carter, C. S. Anterior cingulate
890 cortex, conflict monitoring, and levels of processing. *Neuroimage* **14**, 1302–1308 (2001).
891 59. Hoffman, W. F. *et al.* Cortical activation during delay discounting in abstinent methamphetamine
892 dependent individuals. *Psychopharmacology (Berl.)* **201**, 183–193 (2008).
893 60. Haller, S., Lovblad, K.-O., Giannakopoulos, P. & Van De Ville, D. Multivariate Pattern Recognition
894 for Diagnosis and Prognosis in Clinical Neuroimaging: State of the Art, Current Challenges and
895 Future Trends. *Brain Topogr.* **27**, 329–337 (2014).
896 61. Davatzikos, C., Resnick, S. M., Wu, X., Parmpi, P. & Clark, C. M. Individual patient diagnosis of
897 AD and FTD via high-dimensional pattern classification of MRI. *NeuroImage* **41**, 1220–1227
898 (2008).
899 62. Gonzalez-Gomez, R., Ibañez, A. & Moguilner, S. Multiclass characterization of frontotemporal
900 dementia variants via multimodal brain network computational inference. *Netw. Neurosci.* 1–29
901 (2022).
902 63. Moguilner, S. *et al.* Visual deep learning of unprocessed neuroimaging characterises dementia
903 subtypes and generalises across non-stereotypic samples. *EBioMedicine* **90**, (2023).
904 64. Feis, R. A. *et al.* Single-subject classification of presymptomatic frontotemporal dementia mutation
905 carriers using multimodal MRI. *NeuroImage Clin.* **20**, 188–196 (2018).
906 65. Feis, R. A. *et al.* A multimodal MRI-based classification signature emerges just prior to symptom
907 onset in frontotemporal dementia mutation carriers. *J. Neurol. Neurosurg. Psychiatry* **90**, 1207–
908 1214 (2019).
909 66. Lee, S. E. *et al.* Network degeneration and dysfunction in presymptomatic C9ORF72 expansion
910 carriers. *NeuroImage Clin.* **14**, 286–297 (2017).
911 67. Sheikh-Bahaei, N., Sajjadi, S. A. & Pierce, A. L. Current Role for Biomarkers in Clinical Diagnosis
912 of Alzheimer Disease and Frontotemporal Dementia. *Curr. Treat. Options Neurol.* **19**, 46 (2017).
913 68. O'Connor, C. M. *et al.* Behavioral-variant frontotemporal dementia: Distinct phenotypes with
914 unique functional profiles. *Neurology* **89**, 570–577 (2017).

bioRxiv preprint doi: https://doi.org/10.1101/2024.09.12.612706; this version posted September 16, 2024. The copyright holder for this preprint (which was not certified by peer review) is the author/funder, who has granted bioRxiv a license to display the preprint in perpetuity. It is made available under aCC-BY-NC-ND 4.0 International license.

915 69. Lane, S. D., Cherek, D. R., Rhoades, H. M., Pietras, C. J. & Tcheremissine, O. V. Relationships
916 Among Laboratory and Psychometric Measures of Impulsivity: Implications in Substance Abuse
917 and Dependence. *Addict. Disord. Their Treat.* **2**, 33 (2003).
918 70. Reynolds, B., Ortengren, A., Richards, J. B. & de Wit, H. Dimensions of impulsive behavior:
919 Personality and behavioral measures. *Personal. Individ. Differ.* **40**, 305–315 (2006).
920 71. Odum, A. L. & Baumann, A. A. L. Delay discounting: State and trait variable. in *Impulsivity: The*
921 *behavioral and neurological science of discounting* 39–65 (American Psychological Association,
922 Washington, DC, US, 2010). doi:10.1037/12069-002.
923 72. Schwenke, D., Wehner, P. & Scherbaum, S. Effects of individual and dyadic decision-making and
924 normative reference on delay discounting decisions. *Cogn. Res. Princ. Implic.* **7**, 71 (2022).
925 73. Hirsh, J. B., Morisano, D. & Peterson, J. B. Delay discounting: Interactions between personality
926 and cognitive ability. *J. Res. Personal.* **42**, 1646–1650 (2008).
927 74. Spisak, T., Bingel, U. & Wager, T. Replicable multivariate BWAS with moderate sample sizes.
928 *bioRxiv* 2022–06 (2022).
929 75. Marek, S. *et al.* Reproducible brain-wide association studies require thousands of individuals.
930 *Nature* **603**, 654–660 (2022).
931 76. Sanchez-Roige, S. *et al.* Genome-wide association study of delay discounting in 23,217 adult
932 research participants of European ancestry. *Nat. Neurosci.* **21**, 16–18 (2018).
933

A. General analytic approach

Development of a brain signature predicting log(k) (Study 1)

Predictors: GMD maps

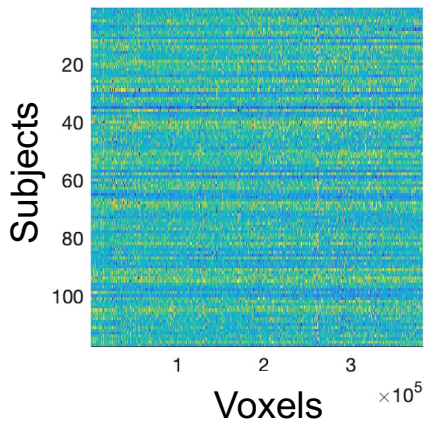

Component reduction

LASSO regression

Outcome: log(k)

LASSO-PCR with 10-fold cross-validation

Training on:

90% of participants

Test on hold-out:

10% of participants

X10

Prediction validity assessment (permutation tests)

Resulting whole-brain pattern
after voxel weight reconstruction

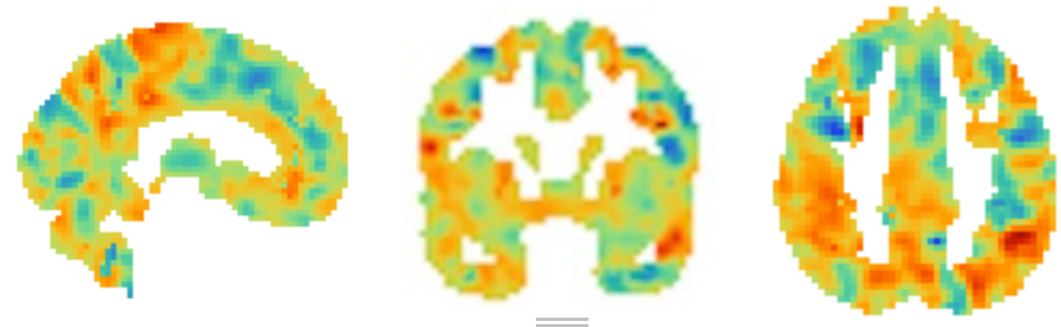

Application to new subjects in independent samples (Studies 2 & 3)

GMD maps

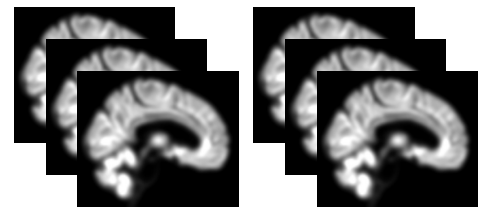

Dot product

Brain-predicted log(k)

Prediction validity assessment

B. Delay discounting paradigms and prediction validity assessment

STUDY 1

N = 117 healthy adults (men)

Money delay discounting task

Actual log(k)

Urgency trait (I-8)

Predicts ?

Brain-predicted log(k)

STUDY 2

N = 166 healthy adults

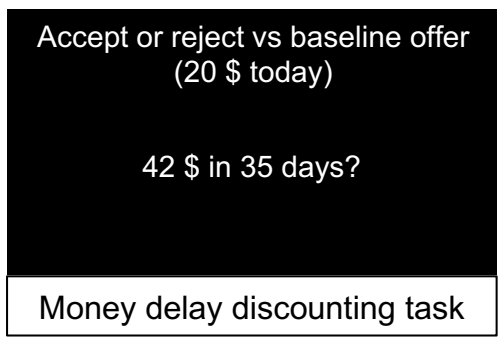

Money delay discounting task

Actual log(k)

Urgency trait (UPPS)

Predicts ?

Brain-predicted log(k)

STUDY 3

N = 24 bvFTD patients & 18 matched controls

Money delay discounting task

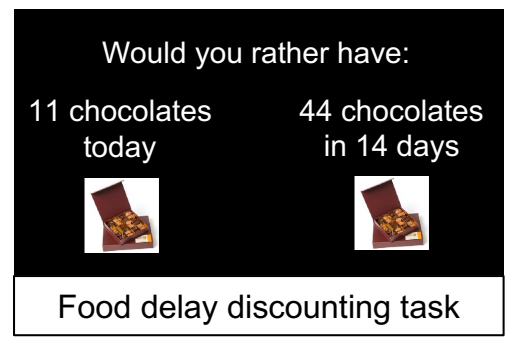

Food delay discounting task

Actual log(k) money - Actual log(k) food

Patient vs Control

Patient's inhibition deficit & executive deficit

Predicts ?

Brain-predicted log(k)

Validity of brain-based predictions of impulsivity in healthy participants

Study 1 – Prediction of delay discounting

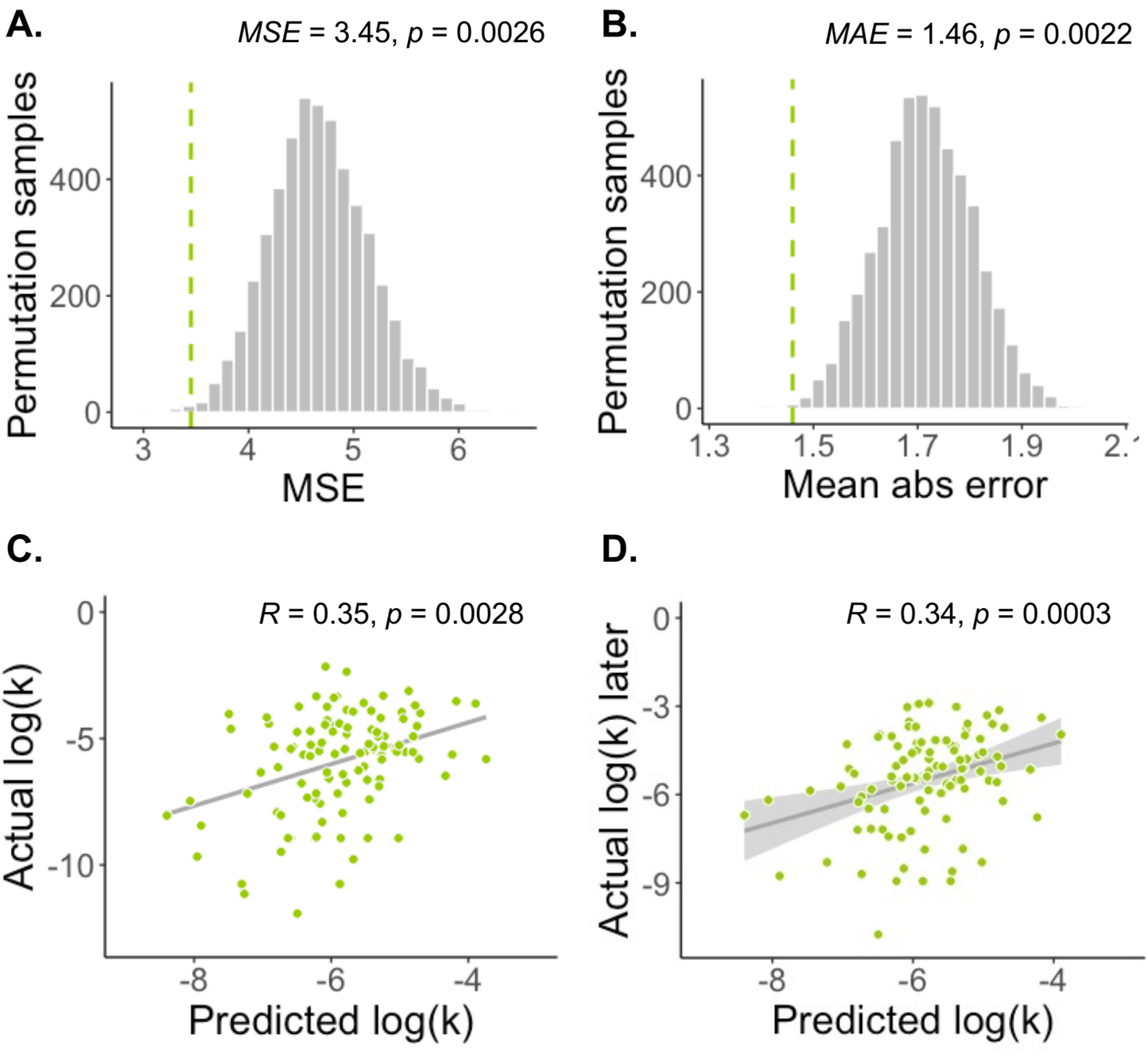

Study 1 – Prediction of urgency

Study 2 – Prediction of urgency

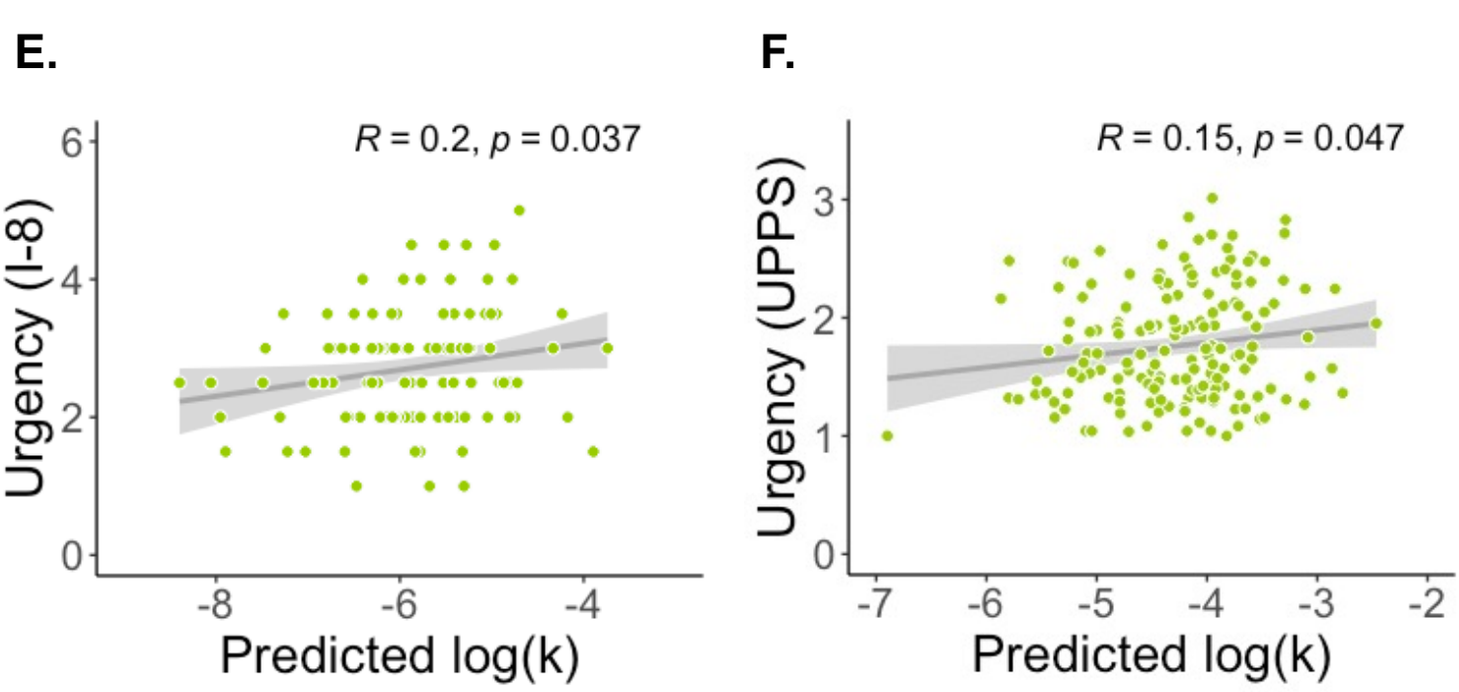

Validity of brain-based predictions of impulsivity in patients with bvFTD matched with controls (Study 3)

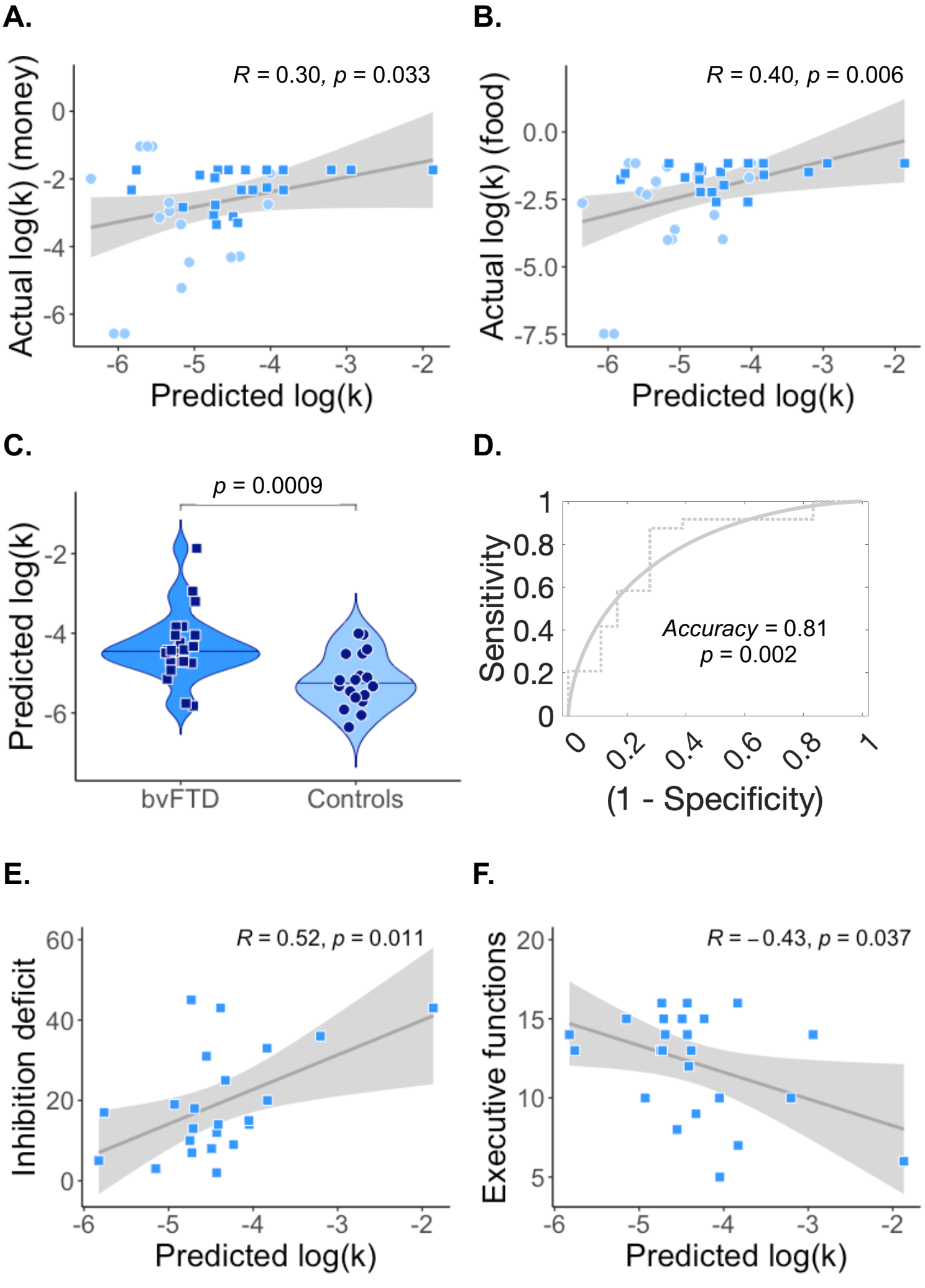

Study 1: Spatial distribution of weights in the structural brain pattern predicting delay discounting

A. Thresholded weights of the brain pattern after bootstrapping

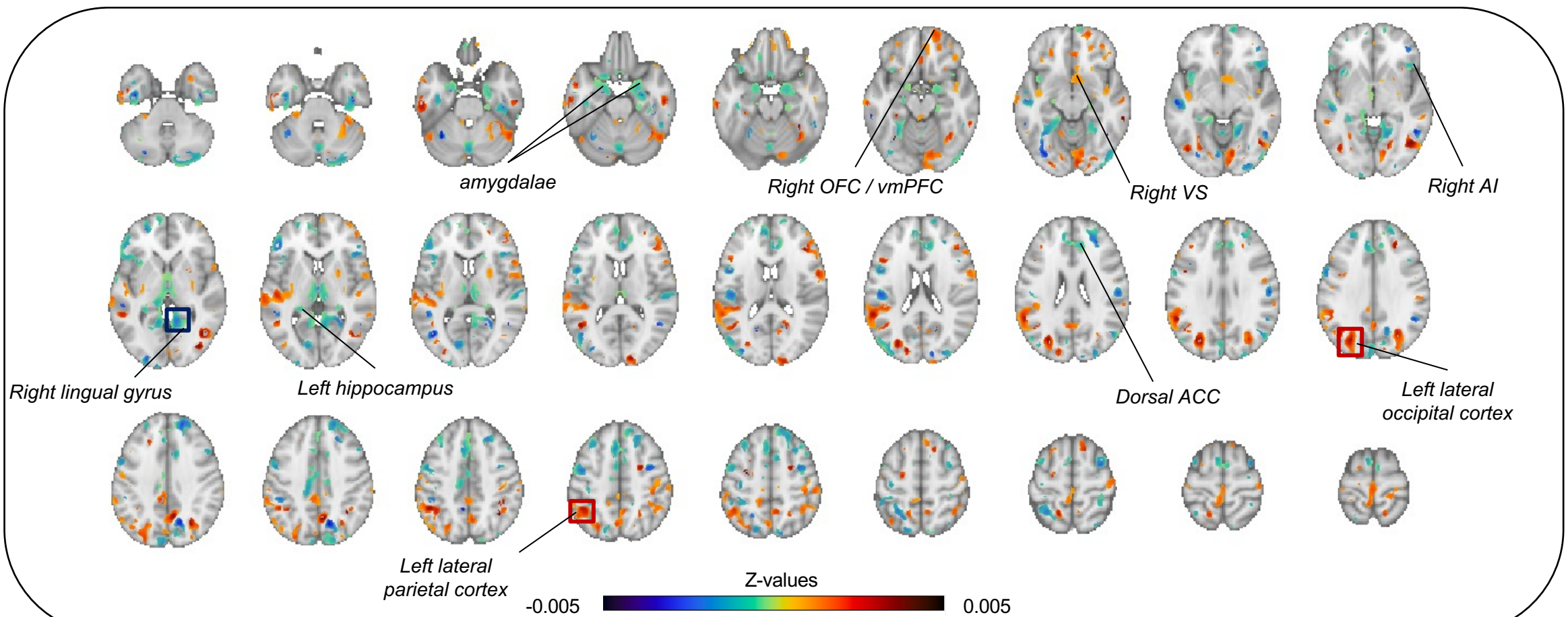

B. Spatial similarity of the brain pattern with meta-analytic maps

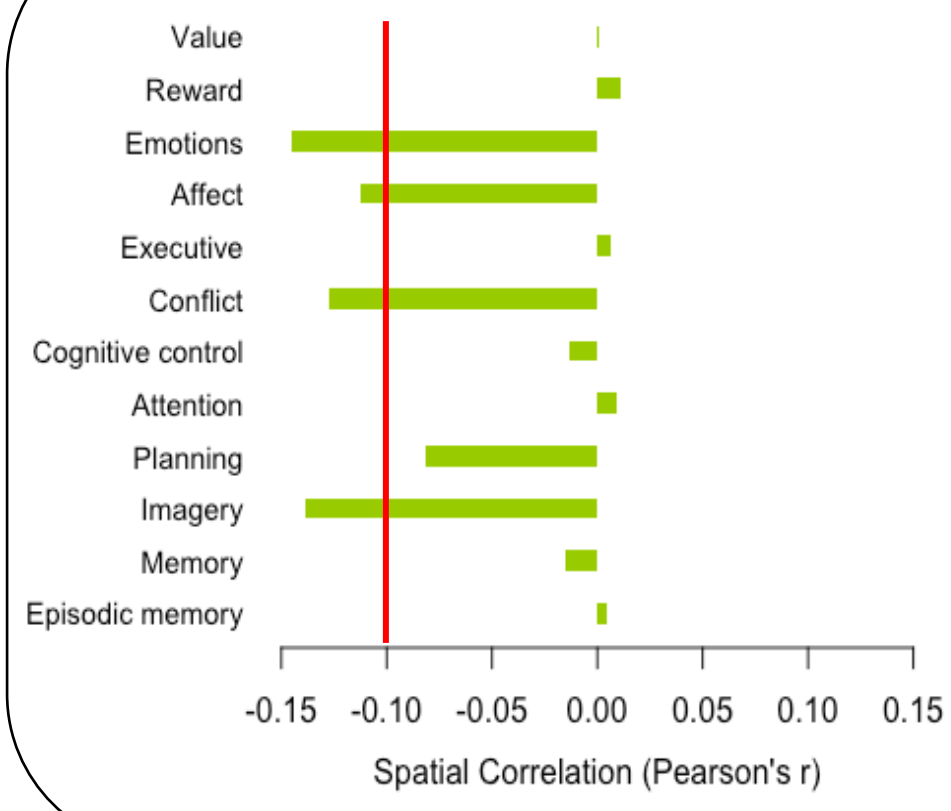

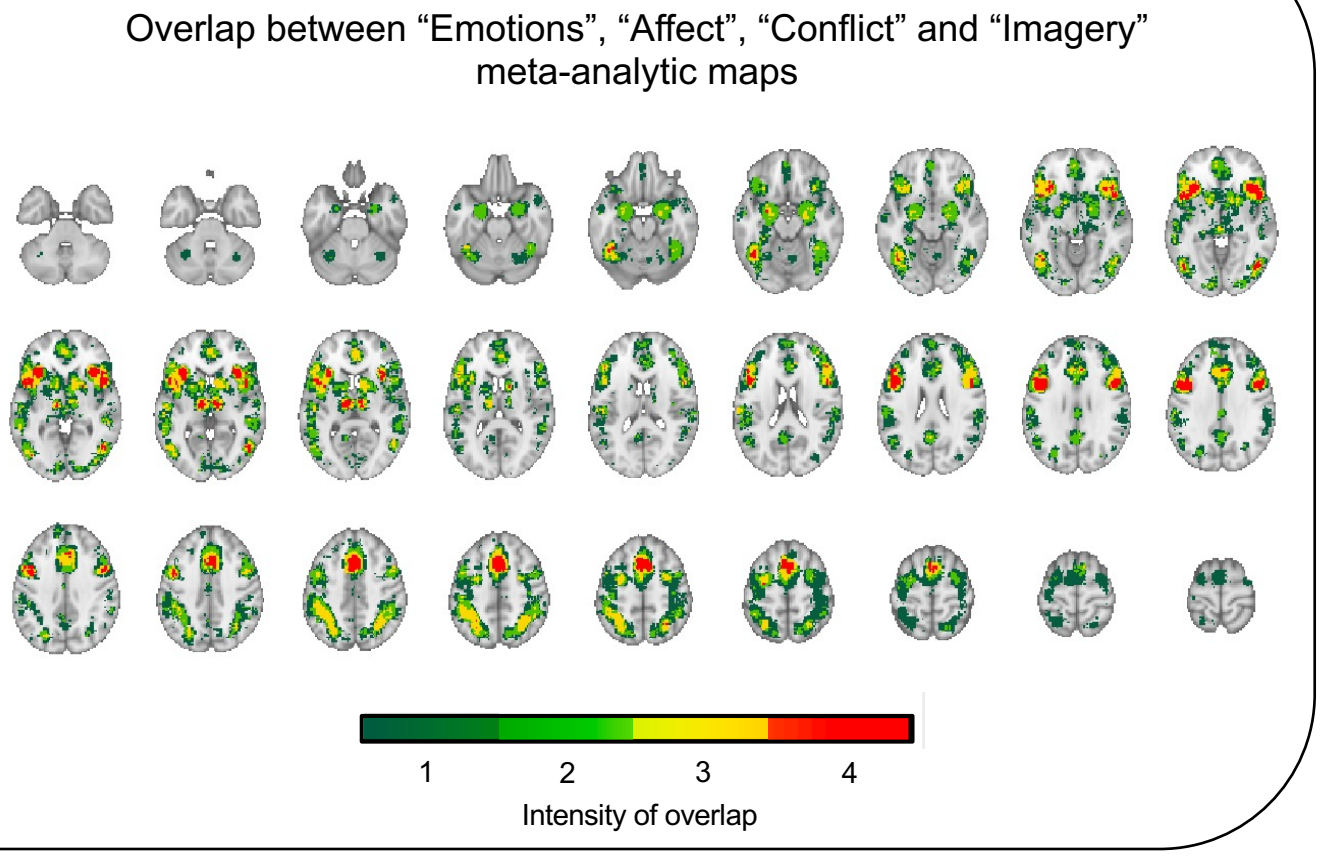

Study 3: Spatial distribution of brain regions contributing to higher predicted delay discounting in bvFTD patients

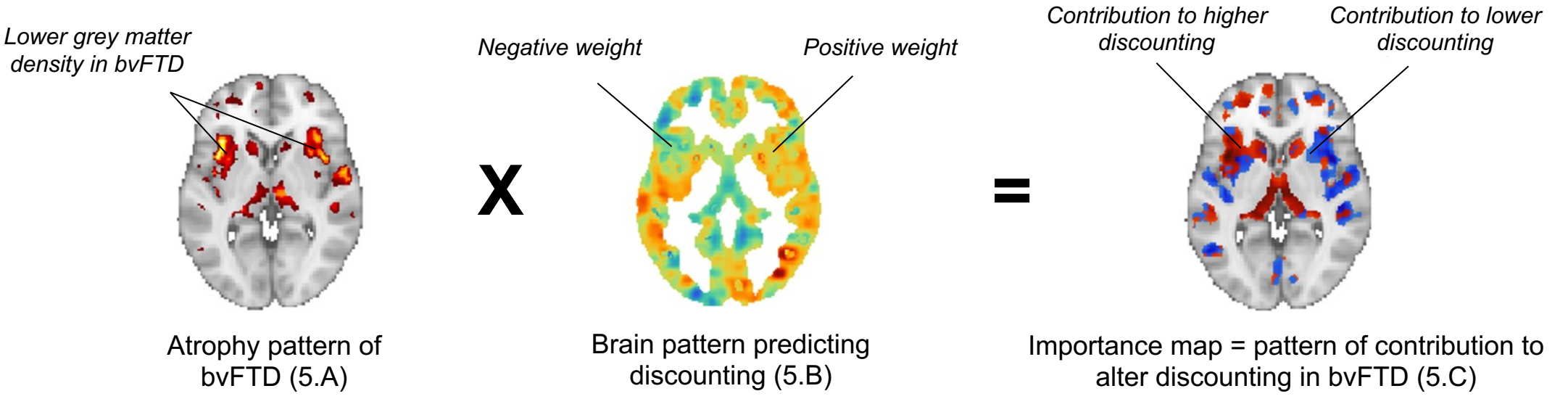

A. Thresholded *T*-map of bvFTD vs Controls contrast (bvFTD<Controls) on whole-brain grey matter density

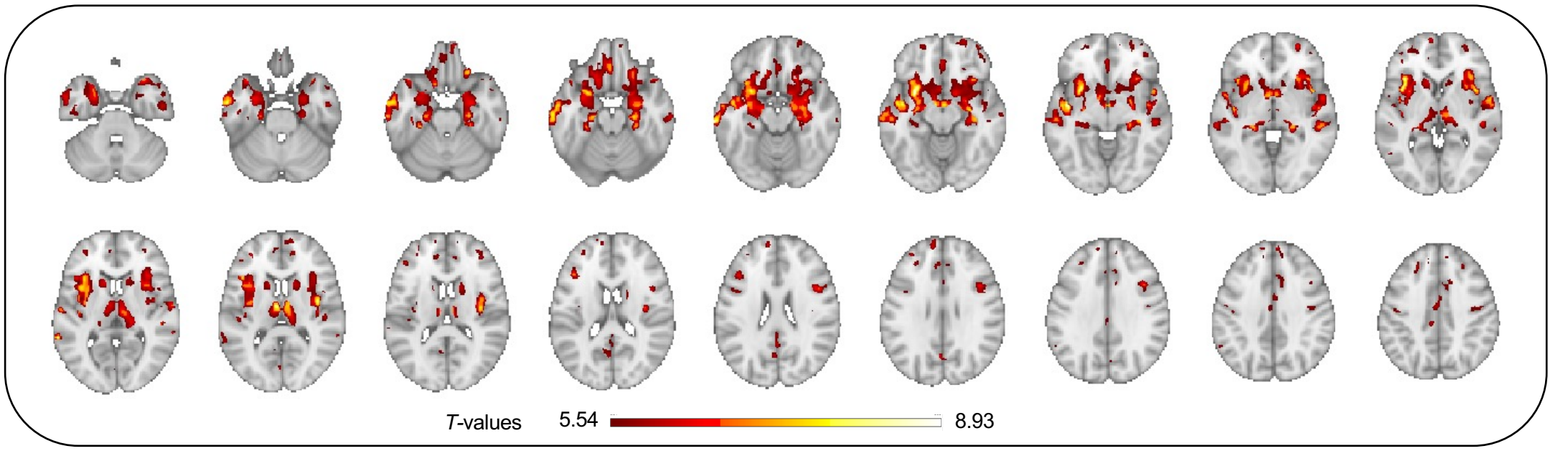

B. Whole-brain weight map of the structural brain pattern predicting delay discounting

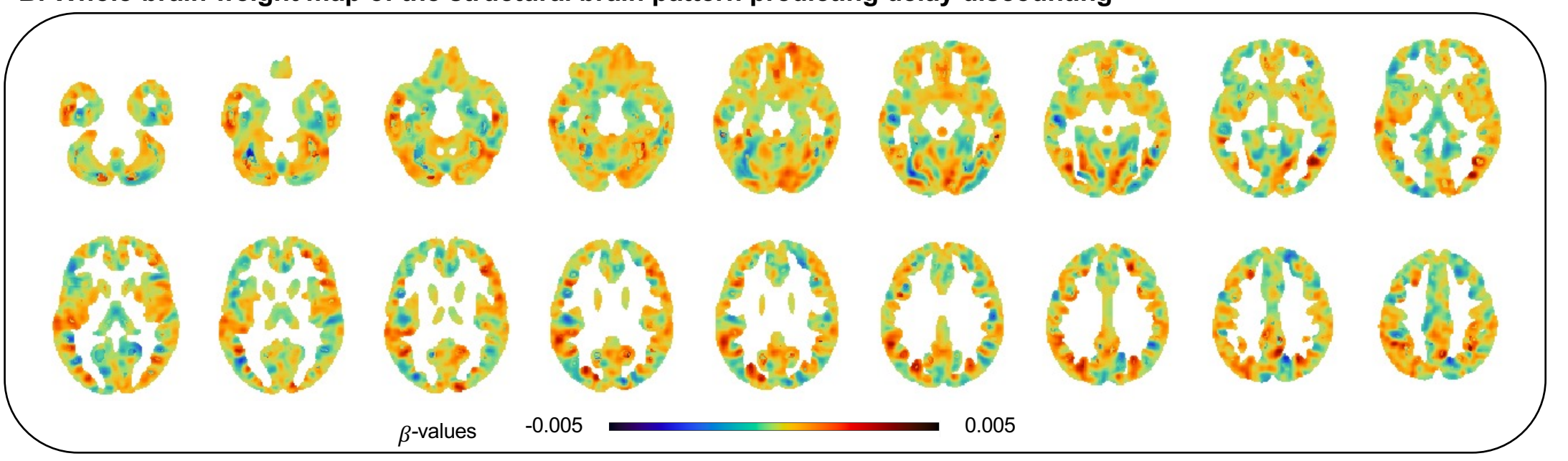

C. Thresholded *T*-map of bvFTD vs Controls contrast (bvFTD>Controls) on whole-brain importance map